

Introduction of Photopolymerization Technology and Application

Xianglong He¹, Liheng Zang², Yangyang Xin³, and Yingquan Zou¹

¹Beijing Normal University College of Chemistry

²Baoding Lucky Innovative Materials Co Ltd

³Hubei Gurun Technology Co Ltd

March 28, 2023

Abstract

Photopolymerization as an energy-saving and environment-friendly technology has been applied in many fields and developed continuously since the middle of the 20th century. Today, photopolymerization technology is ubiquitous in every aspect of our lives. This review starts from the principle of photopolymerization reaction, introduces the process of photopolymerization, initiation mechanism of photoinitiators and three kinds of polymerization methods according to the wavelength of irradiation source. Subsequently, review focuses on the application of photopolymerization technology in thiol-based click reaction, 3D printing, photoresist, hydrogels and other fields, so as to demonstrate its irreplaceable role in the present.

Introduction of Photopolymerization Technology and Application

Xianglong He ^a, Liheng Zang ^b, Yangyang Xin ^c, *, Yingquan Zou ^a, *

^a *College of Chemistry, Beijing Normal University, Beijing, 100875, People's Republic of China*

^b *Baoding Lucky Innovative Materials Co., Ltd, Baoding, 071000, People's Republic of China*

^c *Hubei Gurun Technology Co., Ltd, Jingmen, 448000, People's Republic of China*

Abstract

Photopolymerization as an energy-saving and environment-friendly technology has been applied in many fields and developed continuously since the middle of the 20th century. Today, photopolymerization technology is ubiquitous in every aspect of our lives. This review starts from the principle of photopolymerization reaction, introduces the process of photopolymerization, initiation mechanism of photoinitiators and three kinds of polymerization methods according to the wavelength of irradiation source. Subsequently, review focuses on the application of photopolymerization technology in thiol-based click reaction, 3D printing, photoresist, hydrogels and other fields, so as to demonstrate its irreplaceable role in the present.

1. Introduction to photopolymerization.

As an environmentally friendly technology, photopolymerization in which liquid monomers or oligomers are transformed into solid materials under irradiation of light (ultraviolet, visible or infrared light) holds these advantages of low volatile organic compounds (VOC), fast curing, energy saving, environmental protection, and low temperature compared with traditional thermal polymerization.^[1-6] In addition, photopolymerization is widely used in many fields due to its unique “5E” properties (efficiency, enabling, economical, energy saving and environmental friendly).^[3, 7-12] The history of photopolymerization can be traced back to the 19th century when people observed that styrene polymerized into glassy resin under light. Ostromislenski,

the first researcher of photopolymerization, discovered that the number of constitutional units of product far exceeded the number of photons absorbed in photopolymerization reaction of vinyl bromide, and concluded that the reaction was chain reaction.^[13] The 1960s was the heyday of basic research on photochemistry, its theory gradually improved, and began to be widely applied to actual industrial production.

A complete photopolymerization system generally consists of monomer, oligomer and photoinitiator (PI), all components are indispensable.^[14] Monomers, also known as active diluents, can reduce the viscosity of polymerization system and improve solubility, more importantly, they contain one or more functional groups that can participate in the polymerization reaction such as double bonds, epoxy, oxetane, thiol, etc. Oligomers, whose molecular weights range from several hundred to tens of thousands, have high viscosity and also contain some polymerizable functional groups to participate polymerization. The proportion of monomers and oligomers is large in whole polymerization system, and the properties of polymerization materials are largely determined by them. PI, as an essential component accounting for 1-10 wt % of photopolymerization system, can produce active species under irradiation of light to initiate polymerization reaction, which has great influence on the rate of photopolymerization and the performance of polymerization material.^[15-16]

The procedure of the photopolymerization reaction is exhibited in Figure 1, firstly, PI of ground state undergoes electron transition to excited state under irradiation of light, then generate active species, which are free radicals or cations generally. Active species can interact with functional groups of monomers or oligomers to initiate chain reactions, resulting in the formation of polymer.

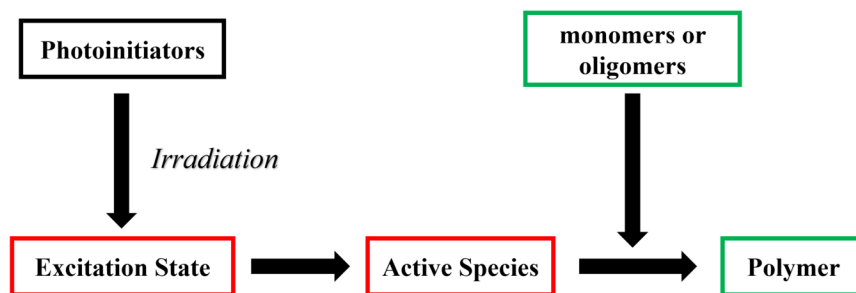


Figure 1 The process of photopolymerization reaction.

2. Photoinitiator of photopolymerization.

PI plays an extremely important role in photopolymerization reaction, it undergoes a series of complex physical or chemical changes in initiating process.^[17-19] As is shown in Figure 2, PI absorbs light, then is excited from ground state (S_0) to singlet state (S_1) which could be returned to ground state by fluorescence emission or nonradiative deactivation, also may reach to triplet state (T_1) by intersystem crossing (ISC). Similarly, PI of triplet state can return to ground state by phosphorescence or nonradiative deactivation as well. When active species are generated by cleavage or hydrogen abstraction of PI in triplet state, photopolymerization can be initiated.

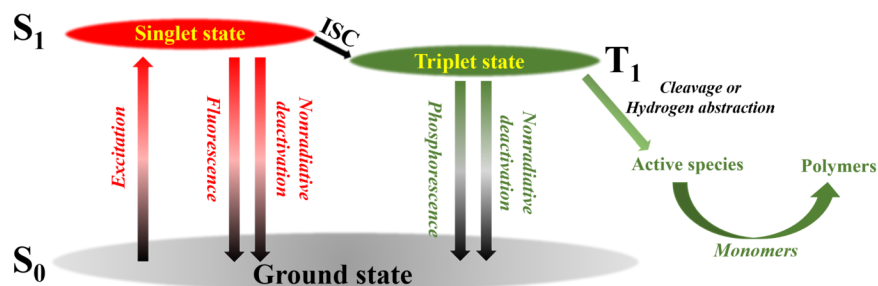


Figure 2 Initiation mechanism of photoinitiator.

According to the different absorbance wavelength, PI can be divided into ultraviolet (UV, mainly below 400 nm), visible light (generally in the range of 400 nm to 700 nm) and near-infrared (NIR, usually greater than 700 nm) PI.^[20-22] Besides, from the perspective of generated active species, PI can be divided into radical type and cationic type, in which radical type composed of cleavage type (Norrish I) and hydrogen abstraction type (Norrish II).^[15, 23-24] The classification of PI is displayed in Figure 3.

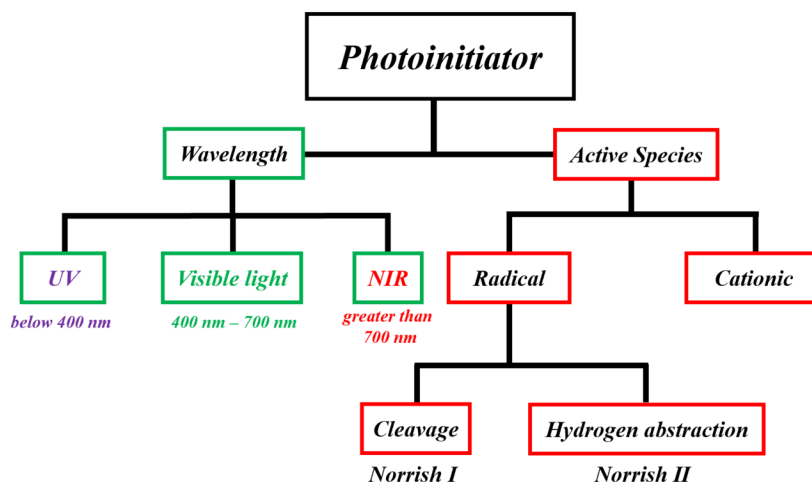


Figure 3 Classification of photoinitiator.

2.1. UV photoinitiator

The earliest species of PIs, mainly absorb UV light to achieve initiation, have been widely employed in numerous fields of UV photopolymerization for many years. Firstly, the cleavage type (Norrish I), refers to formation of radicals by homolytic reaction of weak covalent bond in molecular, includes these species of benzils, benzoin, oxime esters and so on.^[4-5, 10, 25-26] Figure 4 presents several structures of commonly-used cleavable UV PIs such as 2-hydroxy-2-methylpropiophenone (1173), 1-hydroxycyclohexyl phenylketone (184), 2,2-dimethoxy-2-phenylacetophenone (DMPA), 2-hydroxy-4'-(2-hydroxyethoxy)-2-methylpropiophenone (2959), methyl benzoylformate (MBF), benzil, diphenyliodonium (Iod), 2-benzyl-2-(dimethylamino)-4'-morpholinobutyrophenone (369), phenylbis(2,4,6-trimethylbenzoyl)phosphine oxide (BAPO), diphenyl(2,4,6-trimethylbenzoyl)phosphine oxide (TPO), ethyl (2,4,6-trimethylbenzoyl) phenylphosphinate (TPO-L), oxime esters OXE-10 and OXE-02, and cleavage mechanism of PI 1173.^[27] Most

UV PIs of cleavage type undergo one-step cleavage to polymerize the monomers except oxime esters which requires two-step cleavage.

Figure 4 Structures of commonly-used cleavable UV PIs, and cleavage mechanism of 1173.

Different from cleavage type, the hydrogen abstraction type PIs produce radicals by interacting with hydrogen donors, then triggers photopolymerization reaction.^[23, 28] In some cases, hydrogen abstraction type PIs with outstanding light absorption can also sensitize other PIs with weak light absorption, they can be called photosensitizer. Figure 5 records some structures of commonly-used hydrogen abstraction type UV PIs and photosensitizers such as benzophenone (BP), 4,4'-bis(diethylamino) benzophenone (EMK), isopropyl thioxanthone (ITX), 9,10-dibutoxyanthracene (DBA) , and initiation mechanism of BP and donor photoinitiating system.^[27] In addition, several commonly-used hydrogen donors are also exhibited in Figure 5, such as N-phenylglycine (NPG), ethyl 4-dimethylaminobenzoate (EDAB), triethanolamine (TEOA), N-methyldiethanolamine (MDEOA), 2-mercaptobenzothiazole (2-MBTA), 2-mercaptobenzimidazole (2-MBMA) and 2-mercaptobenzoxazole (2-MBXA).

Figure 5 Structures of commonly-used UV PIs of hydrogen abstraction type and several hydrogen donors, initiation mechanism of BP/doner system.

Both types of PIs possess their own characteristics, for cleavage type, rapid initiation and one-component are advantages in practical application,^[29] for hydrogen abstraction type, two-component PIS can effectively relieve the problem of oxygen inhibition, and is generally multifunctional.

2.2. LED photoinitiator

The traditional high-pressure mercury lamp, as the light source of UV photopolymerization, has some shortcomings such as generation of ozone, toxic mercury, short service life and large consumption of energy, which lead to its limitations in practical application. Recently, there has a tendency that the light source of photopolymerization has been moving from UV toward near-UV or visible light using light-emitting-diodes (LEDs).^[5] LEDs possess many merits such as higher-operating efficiency, long service life, low cost, safety, and environmentally friendly,^[3, 6-7, 11, 30-43] as a result, LED photopolymerization has boomed in recent years. Whereas the absorption wavelengths of most traditional UV PI usually are shorter than 365 nm, and do not match with the emission wavelengths (usually higher than 365 nm) of LEDs, so most of the commercially available UV PI cannot be used for LED-induced photopolymerization.^[1, 30] Therefore, the development of PI suitable for LED light sources is necessary.

At present, the LED PI of cleavage type reported mainly include TPO, BAPO, ITX, coumarin-based oxime esters,^[1, 16, 43] naphthalimide sulfur ether,^[23, 29] glyoxylates,^[3, 31, 44-45] and acylgermanes,^[46-48] and so on, the relevant structural formulas are shown in Figure 6 – Figure 9. LED PI of hydrogen abstraction or photosensitizers reported mainly include anthraquinone derivatives,^[35-36, 49] cyclohexanone derivatives,^[37, 50] cinnamoylformate derivatives,^[7] porphyrins derivatives,^[51-52] and so on, the relevant structural formulas are shown in Figure 10 – Figure 13.

Figure 6 Several chemical structures of coumarin-based oxime esters.

Figure 7 Several chemical structures of naphthalimide sulfur ether.

Figure 8 Several chemical structures of glyoxylates derivatives.

Figure 9 Several chemical structures of acylgermane derivatives.

Figure 10 Several chemical structures of anthraquinone derivatives.

Figure 11 Several chemical structures of cyclohexanone derivatives.

Figure 12 Several chemical structures of cinnamoylformate derivatives.

Figure 13 Several chemical structures of porphyrins derivatives.

2.3. NIR photopolymerization

Compared with Ultraviolet (UV) light, Near-Infrared (NIR) light possesses a lower scattering coefficient which is beneficial for a deeper penetration,^[53] and the release of heat is useful for the photopolymerization.^[54] Cyanines are good near infrared light absorbers, can be tailor made by changing the length of methane chain and substitution pattern which can cover a large absorption wavelength region between 700 nm and 1000 nm.^[55] Cyanines can react with iodonium salts to generate free radicals and conjugate acid which can efficiently initiate polymerization of acrylate monomers, epoxides and vinyl ether monomers.^[54, 56-57] Oxime esters can interact with cyanines to initiate photopolymerization of radical monomers.^[58] Alternatively, up-conversion nanoparticles can absorb the NIR laser to emit visible light and UV light which can be absorbed by traditional photoinitiators to trigger photopolymerization.^[59-60] NIR photopolymerization can be applied in digital imaging in Computer to Plate (CtP),^[61] powder coating,^[62] 3D printing,^[63] etc.

3. Application of photopolymerization technology

As a widely-used technology, photopolymerization technology has been used to prepare a variety of products, including coatings, inks, adhesives, printing materials and other applications since Inmont corporation obtained the first UV-curable ink in 1946. In addition to these traditional applications mentioned above, today photopolymerization has been given new applications in thiol-ene click reaction, 3D printing, photoresist, hydrogels and other fields, which will be described in detail below.

3.1. Thiol-ene click reaction

The researches on the reaction between thiols and carbon-carbon double bond has a history of one hundred years.^[64] In 1905, Posner et al. first carried out the researches on the chemical reaction between thiols and enes,^[65-66] then, Kharasch et al. proposed the reaction mechanism of thiols and enes monomers in 1938,^[67] which is still widely accepted today. The photopolymerization mechanism of thiols and enes is demonstrated in Figure 14,^[67-68] first step, the sulfur radicals are generated by the hydrogen abstraction reaction with the free radicals which originate from the cleavage of PIs under irradiation at light sources. The second step, sulfur radicals attack the carbon-carbon double bond and produces alkyl radicals, simultaneously, alkyl radicals can also react with thiols to form sulfur radicals, thus continuously cycling. The third step, radicals combine with each other to terminate the polymerization reaction.

Figure 14 Photopolymerization mechanism between thiols and enes.

The field of click chemistry has been rapid development since Sharpless first proposed the new concept in 2001.^[64, 69] Reaction of click chemistry has many advantages including high yield, short reaction time, solvent tolerance, a wide variety of functional groups, regional and chemical selectivity, insensitivity to oxygen, easy purification and atomic economy up to 100 %.^[64, 70-72] The photopolymerization of thiols and enes carry many of the attributes of click chemistry, and has been applied in many fields such as hydrogels, dental prosthetics, optical materials, bonding, coatings and so on.

In recent years, preparation of organosilicon polymers by UV photopolymerization obtained more and more attention. However, the polymerization reactions between organosilicon monomers modified with acrylate are sensitive to oxygen, resulting in sticky surface and even failure of curing process. On the other hand, the shrinkage rate of the material after curing is very large, which may lead to the deformation of material surface.^[73] Cationic curing is not sensitive to oxygen,^[74] however, its photocuring rate is lower than radical curing. Based on these limitations, Wang et al.^[68] synthesized the novel sulfhydryl functionalized fluorosilicone polymer (PTFPMS-SH) and a series of fluorosilicone polymers (PTFPMS-Vi) with different vinyl contents, then the curing coatings are obtained by thiol-ene click reaction, as displayed in the Figure 15. The results show that the conversion of C=C bond can reach more than 95 % within 5 s, and the obtained fluorosilicone coatings show a transparency greater than 90 %. The contact angle of the coatings

ranges from 100° to 110°, which showing excellent hydrophobicity. In addition, the fluorosilicone coatings show potential application as a protective coating for electronic devices due to excellent corrosion resistance.

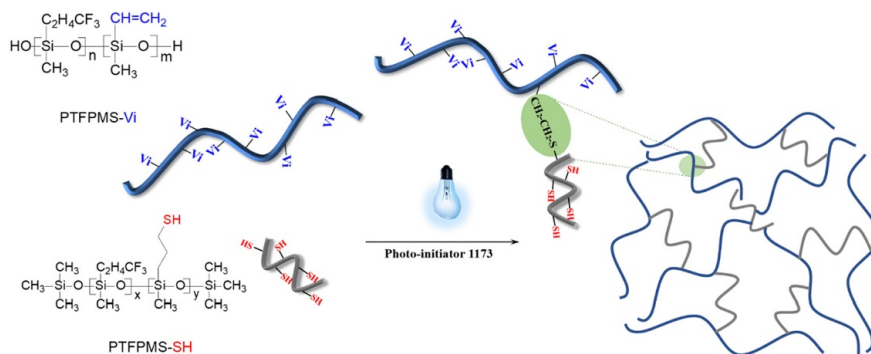


Figure 15 The schematic diagram of photocuring reaction of fluorosilicone coatings.^[68]

About reactive diluents, there are some drawbacks of petroleum-based reactive diluents such as non-renewable feedstock, environmental pollution, skin irritation and poor adhesion in practical application.^[75-76] Therefore, it is a great trend in field of photopolymerization to develop more environmentally friendly and healthy bio-based reactive diluents to substitute petroleum-based one. Yang et al.^[77] synthesized a polyfunctional and renewable reactive diluent tung oil-based methacrylate (TDMM) by amidation, thiol-ene click reaction and esterification, TDMM and acrylated epoxidized soybean oil (AESO) at different proportions to formulate a “green + green” UV-LED curable systems with high bio-content, the chemical structures of AESO and PIs, synthesis route of TDMM are exhibited in Figure 16 and Figure 17, respectively. TDMM/AESO systems show higher T_g but lower thermal stability, better modulus and tensile strength than neat AESO. In addition, the UV-LED cured coatings exhibited excellent physical and chemical properties. In a word, TDMM shows to be an effective reactive diluent, and considered to have good potential in the UV-LED curable coatings.

Figure 16 Chemical structures of AESO and PIs.^[77]

Figure 17 Synthesis route of tung-oil-based acrylate (TDMM).^[77]

As plant phenols from natural origin, cardanol and eugenol are considered renewable raw material for alternatives to fossil feedstock,^[78] and have attracted a lot of attention because their structural versatility, such as C=C bonds, hydroxyl groups, and benzene rings in their structure. Feng et al.^[70] synthesized two allyl monomers (F-CA and F-EU) by cardanol and eugenol underwent esterification reaction with tetrafluoroterephthalic acid, next, a series of biobased polymer networks were obtained via photoclick thiol-ene reaction and thermal treatment between allyl monomers and thiols, the schematic diagram of the preparation of the cardanol-based and eugenol-based thiol-ene polymer networks is displayed in Figure 18. All the polymer networks exhibited high thermal stability (up to 283 °C), excellent solvent resistance and gel content of over 91.36%. Furthermore, the biobased polymer networks displayed a good degradability in alkaline solution on account of the presence of ester bonds and electron-deficient aromatic ring system. The multifunctional biobased thiol-ene polymer networks may have practical applications in many areas such as coating, composites, adhesives, etc.

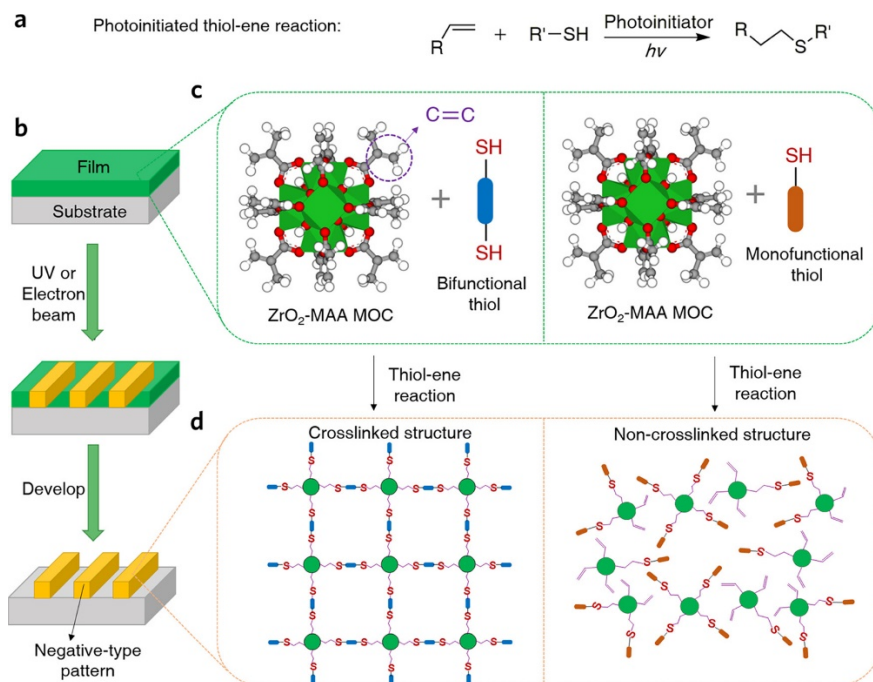


Figure 20 Schematic illustration of thiol-ene reaction and click lithography. (a) Photoinitiated thiol-ene reaction. (b) Representation of the click lithography approach. (c) Resist film composed of ZrO_2 -MAA MOCs and thiol compounds. (d) Crosslinked and non-crosslinked structures formed by radiation-induced thiol-ene click reaction.^[79]

3.2. 3D Printing

Different from traditional manufacturing methods, the three-dimensional (3D) printing techniques were introduced during the 1980s with the aim to fabricate customized/complex objects without the need for molds or machining, also known as additive manufacturing (AM) technology.^[80-82] 3D printing method based on the photopolymerization techniques has been a hot topic in recent years due to many advantages such as highest accuracy, high production efficiency, material utilization rate of nearly 100 % and mild facilities.^[83-84] Therefore, photopolymerization 3D printing have received revitalized attentions in a variety of 3D printing such as stereolithography (SLA),^[85] direct laser writing (DLW),^[86] digital light processing (DLP),^[87] ink jetting,^[88] and real-time curing of DIW.^[63, 89]

Several commercial UV-light-sensitive PIS such as TPO, BAPO, Irgacure 184, and Irgacure 369 were used for the 3D printing processes of photopolymerization under irradiation at UV light.^[35] Whereas, as explained in section 2.2, visible light source has obvious advantages over traditional UV light source, hence the development for novel PIs or PISs for photopolymerization 3D printing induced by visible light is essential. Xiao et al.^[35] investigated a series of disubstituted aminoanthraquinone derivatives which are capable of initiating the radical photopolymerization under irradiation at blue to red LEDs. The chemical structures of the studied disubstituted aminoanthraquinone derivatives (AHAQ, 14-DAAQ, and 15-DAAQ) and additives (Iod, NVK, TEAOH, and R-Br) are shown in Figure 21. 15-DAAQ/TEAOH/R-Br PISs was used for the 3D printing due to the highest capacity to initiate the radical polymerization of acrylates and the 3D resin. It took less than 8 min to print the keyring when using 15-DAAQ/TEAOH/R-Br system under irradiation at polychromatic visible light (400–730) nm with light intensity 3.6 mW cm^{-2} , as a contrast, TPO took 35 min. Markedly, the printing speed was significantly enhanced when using the 15-DAAQ/TEAOH/R-Br as the PISs, which indicates that 15-DAAQ/TEAOH/R-Br system can be used as a promising PIS for fast 3D printing. The experimental 3D printing product using 15-DAAQ/TEAOH/R-Br PISs is shown in the Figure

22.

Figure 21 Chemical structures of the studied disubstituted aminoanthraquinone derivatives and additives.^[35]

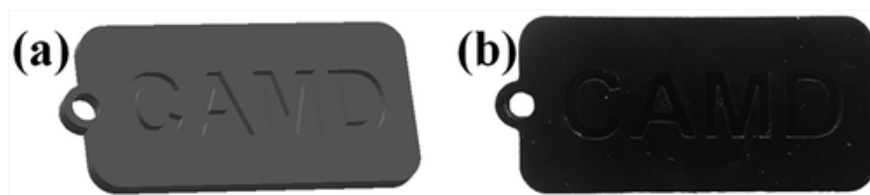


Figure 22 (a) 3D model of keyring and (b) 3D printed keyring (64.0 mm × 30.0 mm × 3.6 mm) using 15-DAAQ/TEAOH/R-Br (0.5%/2%/2%, wt %) as PISs.^[35]

In addition to this, Xiao et al.^[90] also investigated the application of indigo carmine (IDGCM) as a photosensitizer with for 3D printing of photopolymerization. IDGCM possesses excellent good water solubility, visible light sensitivity and biocompatibility, hence it can give the corresponding properties of photopolymerization and 3D printing. The chemical structures of IDGCM, additive, and monomer/oligomers used in corresponding experiments are shown in Figure 23. The indigo carmine-based photoinitiating system induced a rapid photochemical reaction and photobleaching under blue and green LEDs with low light intensity. The photopolymerization system composed of IDGCM/Iod (0.5 %/2 %, wt) and PEGDA 700/deionized water (80 %/20 %, wt) in the presence of 25 mM NaOH can achieve rapid and high-fidelity 3D printing, as shown in Figure 24.

Figure 23 Chemical structures of IDGCM, additive, and monomer/oligomers.^[90]

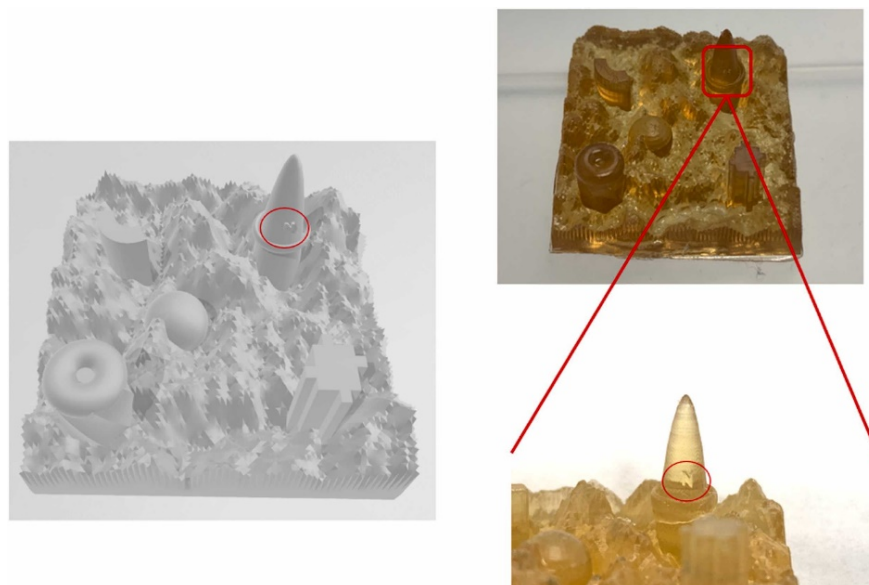


Figure 24. The top view of STL model file and the topography print cured using the PEGDA 700/water (80 %/20 %, wt) in the presence of IDGCM/Iod (0.5 %/2 %, wt) and 25 mM NaOH. (30 × 30 × 15 mm, L × W × H).^[90]

In the process of photopolymerization 3D printing, the light transmitted through the solidified polymer layers is highly likely to trigger undesired lateral photopolymerization during the printing of subsequent layers and therefore leads to deteriorated print resolution.^[91] Nonreactive light absorbers can improve print

resolution by limiting light penetration, however, they also reduce printing speed.^[92] It is a challenging to develop a 3D printing technique with both high print speed and resolution. Xie et al.^[93] designed an efficient 3D printing method by using one ketocoumarin compound, i.e., 3,3'-carbonylbis(7-diethylaminocoumarin) (KCD), as the photosensitizer (also a reactive light absorber) because of its high photoinitiation efficiency, low bleaching capacity and high molar extinction coefficient of photolysis products (limiting light penetration and improving resolution). The processes of generating radicals through photooxidation or photoreduction are shown in Figure 25 a, it is difficult to limit the light penetration due to the obvious blue shift (61nm) of the product KCD ketyl radical in the photoreduction process, which resulting in low resolution and the printed feature could not be identifiable (Figure 25 c). In comparison, the photopolymerization 3D printing based on the photooxidation of KCD that functions as the photosensitizer can simultaneously deliver high print speed (5.1 cm h⁻¹) and high print resolution (23 μm). The method provides a viable solution towards efficient AM by controlling the photoreaction of photosensitizers during photopolymerization.

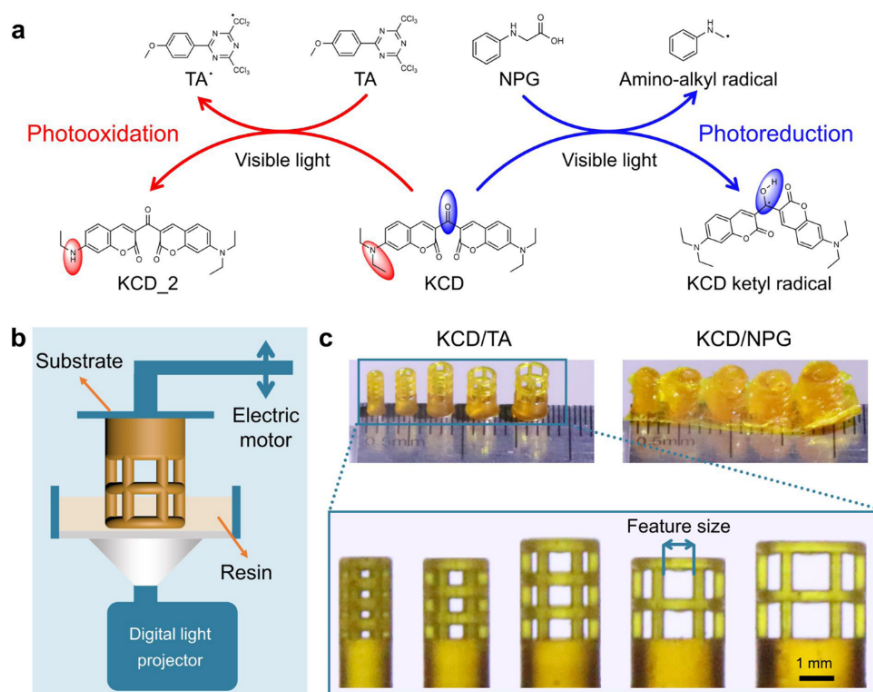


Figure 25 (a) Schematic illustration of the photooxidation of KCD/TA and photoreduction of KCD/NPG upon visible light irradiation, respectively. (b) Schematic illustration of the bottom-up DLP 3D printing. (c) 3D-printed objects photomediated by KCD/TA and KCD/NPG, respectively.^[93]

At present, UV and blue lights are the main irradiation sources in photopolymerization 3D printing.^[94] Despite the convenience offered by UV and blue lights, intensity of short wavelength lights is a trade-off for better mechano-properties by uniformed polymerization and health concern of UV exposure.^[63] Among the photopolymerization methodologies, NIR has a more salient role in rapid deep-curing for its remarkable penetration in various media by employing up-conversion strategies.^[60, 95-96] Liu et al.^[63] reported a NIR photopolymerization 3D printing strategy, and the fusion of NIR photocurable material and DIW 3D printing technology could achieve in-situ curing of thick filament with high penetration. The structure of NIR-induced DIW setup, chemical structures and photoreaction mechanism used in NIR DIW printing, and monitoring of NIR photopolymerization are exhibited in Figure 26. This enables the photocuring of deposited filaments up to 4 mm in diameter, which far exceeding any existing UV-assisted DIW, in addition, the strategy also possesses the capability of parallel fabrication to multi-color filaments and freestanding objects simultaneously.

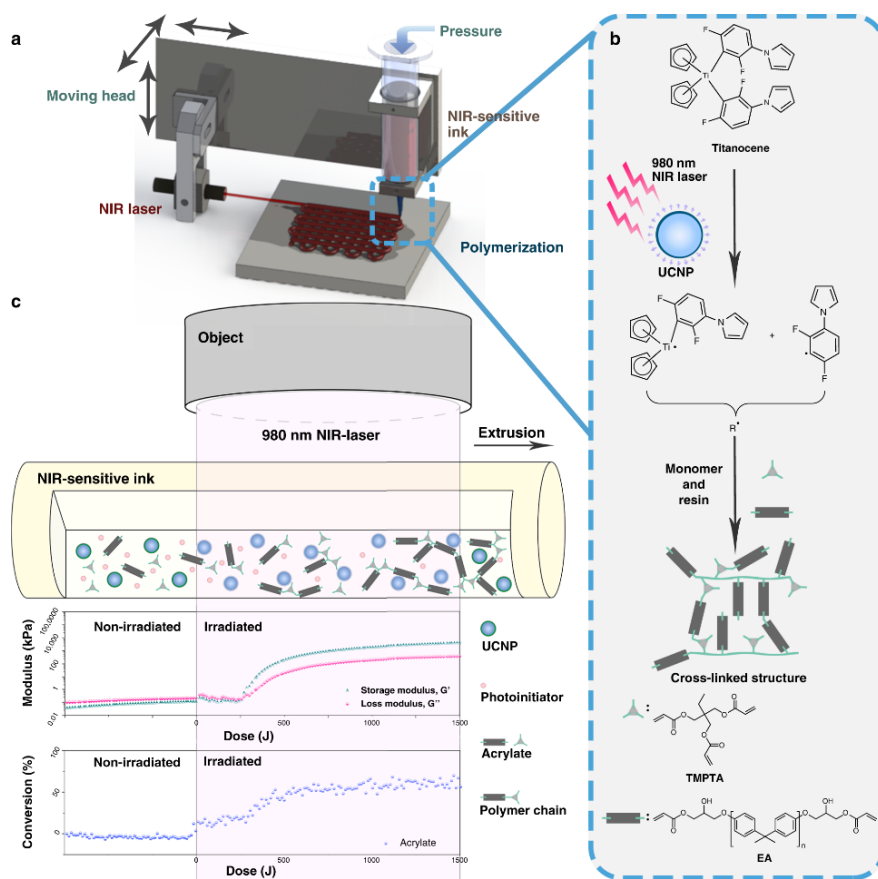


Figure 26 Schematic of NIR-DIW and real-time FTIR photorheology analysis. a Scheme of NIR-induced DIW setup; b structures and reactions applied in NIR DIW printing; c monitoring of NIR-induced photopolymerization by real-time FTIR rheological analysis.^[63]

3.3. Photoresist

As the key of photolithography, photoresist refers to thin film materials whose solubility and adhesion change significantly after exposure by light sources, then the micro-patterns can be obtained through development, etching and other processes.^[97] It is widely employed in the fields of printed circuit boards (PCB),^[98-100] display device,^[101-103] integrated circuit,^[104] and other fine graphics processing. Photoresist can be divided into positive photoresist and negative photoresist on the basis of the area retained after development, in which negative photoresist is photocurable materials. The schematic diagram of photolithography is shown in Figure 27.^[97]

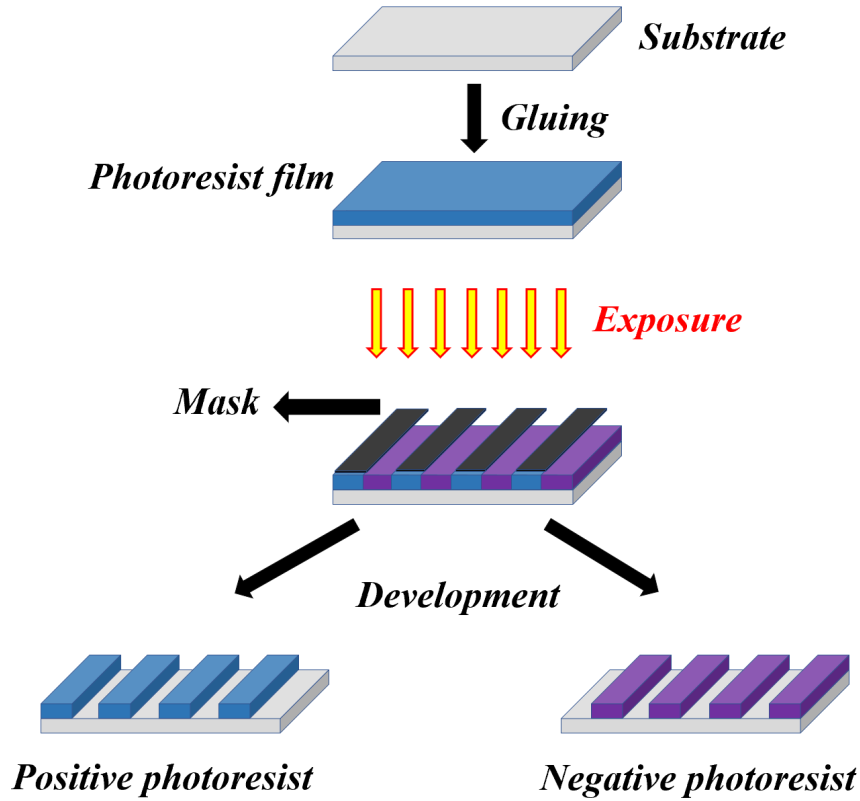


Figure 27 Schematic diagram of photolithography.

Negative photoresist can be divided into photoinitiated radical polymerization (mainly acrylic ester system) and photoinitiated cationic polymerization (mainly epoxy system). The typical negative photoresist consists of PISs, acrylate monomer, resin, additive and solvent, it is mainly used in the field of PCB and display devices.

3.3.1. PCB dry film photoresist

With the rapid development of numerous industries of electronic information such as automotive electronics, artificial intelligence, commercialization of 5G and wearable devices, the Printed Circuit Board (PCB) industry has witnessed a fast growth in recent years. The photoresist used in the PCB industry mainly includes liquid photoresist and dry film photoresist (DFRs). Due to its unique advantages of uniform thickness, controllable, stability, high reliability, easy operation, low energy of exposure and high resolution, DFRs has developed rapidly, and has been widely utilized in PCB manufacturing process.^[105-108] As displayed in Figure 28, the polyester (PET) film, photoresist layer and polyethylene (PE) film from bottom to top together constitute a complete DFRs.^[109] The PET film plays the role of bearing photoresist layer, and PE film is used to avoid the deterioration caused by the contact between photoresist layer and dusts or oxygen, in addition, prevents adhesion between multilayer film.

The photoresist layer of DFRs generally composed of resins, monomers, oligomers, photoinitiators, dyes and other additives.^[109-111] Resin possesses the largest mass ratio in all components of DFRs, and directly determines the resolution, adhesiveness, developing time and flexibility, etc. the most commonly-used PIs for DFRs are hexarylbiimidazole (HABIs) compounds,^[43] among which 2,2-bis(2-chlorophenyl)-4,4,5,5-tetraphenyl-1,2-biimidazole (BCIM) has been broadly employed due to its merits of good efficiency and discoloration property. However, it always cooperates with photosensitizers because the light absorption

capacity of BCIM in near-UV and visible light region is weak.^[112] The structures and photoinitiation mechanism of BCIM/N-phenylglycine (NPG) systems are shown in Figure 29, firstly of all, BCIM will generate imidazole radicals at exposure to light source, which reacts further with NPG to generate carbon-centered radical that can initiate polymerization reaction rapidly.^[112]

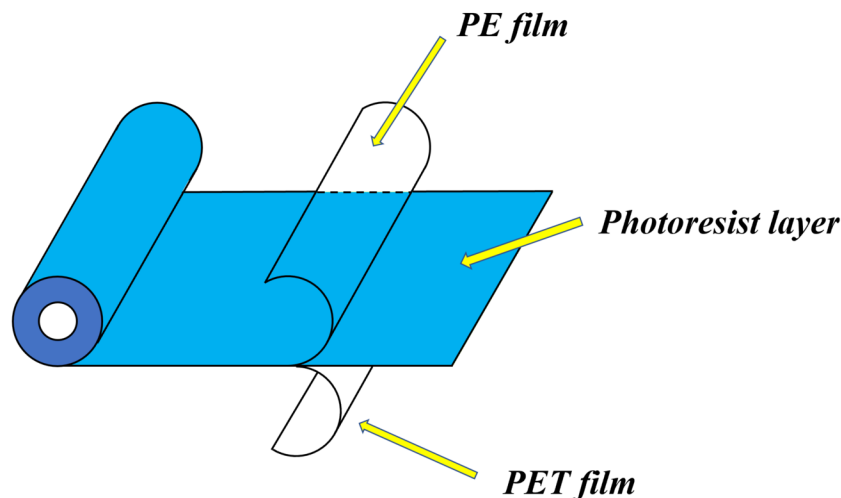


Figure 28 Structure composition of PCB dry film photoresist.

Figure 29 Structures and photoinitiation mechanism of BCIM/NPG systems.

EMK and PSS303 are used as photosensitizer in DFRs formula for many years, however, it is essential to develop more efficient photosensitizers due to the requirements of higher sensitivity and resolution in DFRs. Jiang, et al.^[113-114] reported several novel species of photosensitizers that can be utilized for DFRs, respectively distyrylpyridine derivatives (DSPs) and anthracenes (ANs) derivatives, and their structures are exhibited in Figure 30 and Figure 31. Firstly, among all DSPs, the 24DMOP-DSP has the highest photosensitivity, which was reached 14 mJ.cm⁻² and increased by 150% compared to contrastive commercial coumarin-based DAMC with 35 mJ.cm⁻². The singlet state of DSPs is easily quenched by BCIM, which proves that it is easy to sensitize BCIM then initiate polymerization reaction. Next, for ANs, they possess strong light absorption from 350 nm to 450 nm with high molar extinction coefficients, which can be matched with multifarious light sources. BCIM can be photosensitized by ANs to initiate the polymerization reaction of Hexamethylene diacrylate (HDDA) effectively. The DFRs formula containing ANs/BCIM can obtain fine high-resolution micro-patterns by 405 nm laser direct-writing photolithography.

Figure 30 Chemical structures and synthesis methods of DSPs.^[113]

Figure 31 Chemical structures of ANs.^[114]

Ho, et al.^[112] synthesizes a series of p-substituted NPG derivatives OMe-NPG, Cl-NPG and NO₂-NPG as shown in Figure 32. The OMe-NPG, Cl-NPG and NO₂-NPG have good thermal stability and red-shifted absorption compared with NPG, the photopolymerization performance of trimethylolpropane trimethacrylate (TMPTMA) initiated by BCIM/NPGs systems was tested, the measured conversions sequence is BCIM/NPG (51.7 %) > BCIM/OMe-NPG (41.8 %) > BCIM/Cl-NPG (35.5 %) > BCIM/NO₂-NPG (0 %), which concluded that introduction of substituents may weaken the performance of initiating for NPG.

Figure 32 Structures of N-phenyl glycine (NPG) and NPG derivatives (OMeNPG, Cl-NPG and NO₂-NPG).^[112]

As we know, radicals photopolymerization system possess some defects in practical productions such as apparent volume shrinkage, poor precision and low adhesion.^[115] Contrastively, the cationic photopolymerization system has lower shrinkage, stronger adhesion and hardness, making them particularly suitable for laser photolithography technology which requires high precision and strong adhesion.^[116-118] Based on this, as shown in Figure 33, our group designs and synthesizes a series of cationic photocurable resins which consists of methyl methacrylate (MMA), methacrylic acid (MAA), ethyl methacrylate (EMA) and 3-ethyl-3-(methacryloyloxy) methyloxetane (EMO) by radical copolymerization.^[109] Next, we used these resins to prepare DFRs formulations with radical/cationic dual-curing. The DFR based on the resin which containing 10 wt % of EMO has the highest photosensitivity (11 mJ/cm², ST = 20/41) and 20 μm (ST = 20/41) can be obtained by using this resin. In conclusion, the DFRs that contain cationic photocurable resin may have potential application in PCB field for creating high resolution patterns.

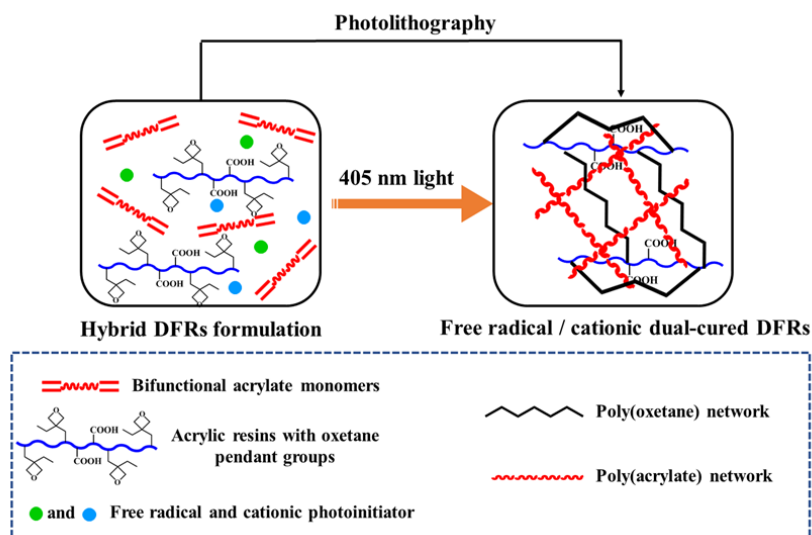


Figure 33 A proposed photolithography based on radical and cationic dual-curing photoresists.^[109]

The most commonly-used photoresist of cationic photopolymerization is SU-8, which is a UV photoresist product specially designed for Micro-Electro-Mechanical System applications with high aspect ratio.^[119-120] The main component of SU-8 is a multi-function group and multi-branch epoxy resin, which is synthesized by the condensation reaction of bisphenol and glycerol ether, ideal structural formula of SU-8 is shown in Figure 34.^[121] The PIs used in SU-8 series photoresist is generally an onium salt, mainly sulfonium salt, which can produce a strong acid under irradiation to polymerize the epoxy groups.^[122]

Figure 34 Ideal structural formula of SU-8.

3.3.2. UV nanoimprint lithography photoresist

As an emerging high-resolution patterning method, nanoimprint lithography (NIL) provides a technology that could replicate the nanoscale patterns below 10 nm, and is a promising solution to the restriction of exposure wavelength in photolithography.^[123] NIL has overcome tremendous challenges over the past 20 years to become a realistic method for commercial semiconductor production.^[124] UV-nanoimprinting lithography (UV-NIL) is regarded as the new next-generation lithography technique due to the advantages of high throughput, good resolution, and low manufacturing cost, room-temperature operation,^[123, 125] and has been receiving increasing attention in many fields such as electronic, photonic, LED, magnetic and semiconductor devices.^[125-127]

The cross-linker plays a very important role in the component of traditional UV-NIL photoresist, which determines the mechanical and chemical resistance to a certain extent. However, the high cross-linked structure is difficult to strip from the mold of UV-NIL, conversely, the linear structure displays better solubleness in solvent.^[128] Yin et al.^[129] designed a UV-NIL resist in which the structure contains photoreversible coumarin derivative as degradable cross-linker. The chemical structures of degradable cross-linker (AHAMC), monomer phenoxy ethyleneglycol acrylate (AMP-10G), and the mechanism of photodimerization and photocleavage of the dimer-coumarin-bridged polymer are exhibited in Figure 35. Through photodimerization of coumarin moieties under irradiation at 365 nm UV light, and photocleaved by 254 nm UV light, the crosslinking and uncrosslinking can be implemented to protect the mold.

Based on the photoreversible coumarin derivatives, Wei et al.^[130] reported a pH-UV dual-responsive photoresist for UV-NIL that improves mold release, the chemical structures of the photoreversible cross-linker 5,7-diacryloyloxy-4-methylcoumarin (DAMC), acrylic anhydride (ALA), 3,6-dioxa-1,8-dithiooctane (EGDT) and the PI DMPA for the dual-responsive resist are displayed in Figure 36. The mechanism of degradation for dual-responsive resist is displayed in Figure 37, the cross-linked networks can be photocleaved by 254 nm UV light and degraded in alkaline aqueous solution, which contributes to protect UV-NIL mold and reduce damages in process of imprinting patterns.

Figure 35 Mechanism of photodimerization and photocleavage of the dimer-coumarin-bridged polymer.^[129]

Figure 36 Chemical structures of each component for the dual-responsive resist.^[130]

Figure 37 Mechanism of degradation for dual-responsive resist.^[130]

Volume shrinkage is inevitable due to the van der Waals distance before polymerization becomes the covalent distance after polymerization, consequently, volume shrinkage has a negative impact on the patterns transfer in UV-NIL.^[131] It is necessary and meaningful to reduce volume shrinkage in UV-NIL field. Based on the disulfide bond of reducing volume shrinkage and endowing materials with the degradability. Sun et al.^[125, 132] synthesized two disulfide bond-containing acrylate monomers 2,2-dithiodiethanol diacrylate (DTDA) and disulfanediy bis (1,4-phenylene) diacrylate (ADSDA) used for UV-NIL. The chemical structures of DTDA and ADSDA are exhibited in Figure 38. For the photoresist containing DTDA, it underwent a repeated “contraction–expansion–contraction” volume-modulatory process during the polymerization because of the dynamic reversible property of homolysis and recombination of disulfide bonds, which was conducive to releasing stress and reducing volumetric shrinkage. Such as the DTDA/MMA/IOBA system, the minimum rate of volume shrinkage can drop to 0.93 %. The mechanism of reducing volume shrinkage is displayed in Figure 39.

Figure 38 Chemical structures of DTDA and ADSDA.^[125, 132]

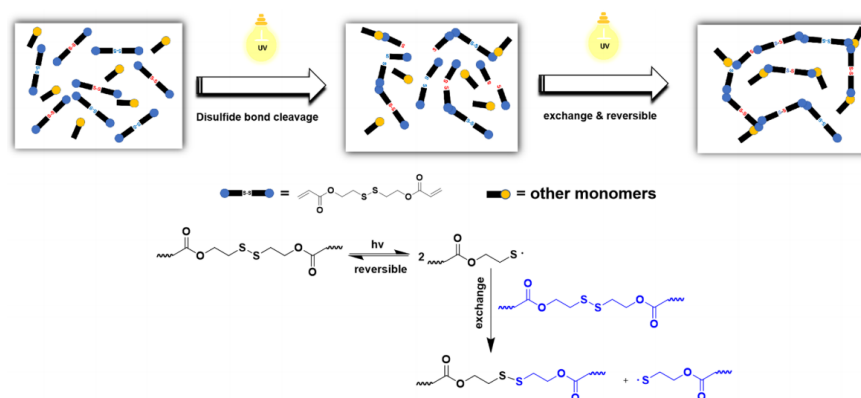


Figure 39 Mechanism of reducing volume shrinkage based on the reversible disulfide-bond.^[125]

For the photoresist system containing ADSDA, it does not contain any additional PI due to the arylthiyl radical generated by ADSDA possesses a good capability of initiating photopolymerization. The photoresists with ADSDA exhibited a capability of photopolymerization in the absence of PI, and their double bond conversion can reach up to 86 %, at the same time, the volume shrinkage of the polymerized photoresists with ADSDA could even drop to 0.56 % owing to the “breakage–recombination” reversible reaction of disulfide bonds.

Oxygen inhibition of acrylate-based resists limits the potential of UV-NIL for high throughput, however, the photopolymerization system of thiol–ene leads to extremely little oxygen inhibition, simultaneously, it also has the properties of high monomer conversions, low shrinkage, homogeneous mechanical properties. Besides, the etch resistance and thermal stability of cured resist are important because these properties allow good pattern transfer. The inorganic polyhedral oligomeric silsesquioxane (POSS) combines many desirable properties as an NIL photoresist such as optical clarity, high thermal stability, high density, high Young’s modulus, and a low dielectric constant, meanwhile, it does not affect the resolution of the NIL pattern.^[133-135] Based on this, Yin et al.^[136] developed a novel POSS containing mercaptopropyl (POSS-SH), the structures of each component of the hybrid UV-NIL resist are displayed in Figure 40. POSS-SH can enhance the thermal properties, dimensional stability and etching resistance of UV-NIL resist, and reduce the volume shrinkage. The hybrid resist can obtain the high aspect ratio patterns as showed in Figure 41, which is beneficial for graphics transfer onto Si.

Figure 40 Chemical structures of each component of the hybrid UV-NIL resist.^[136]

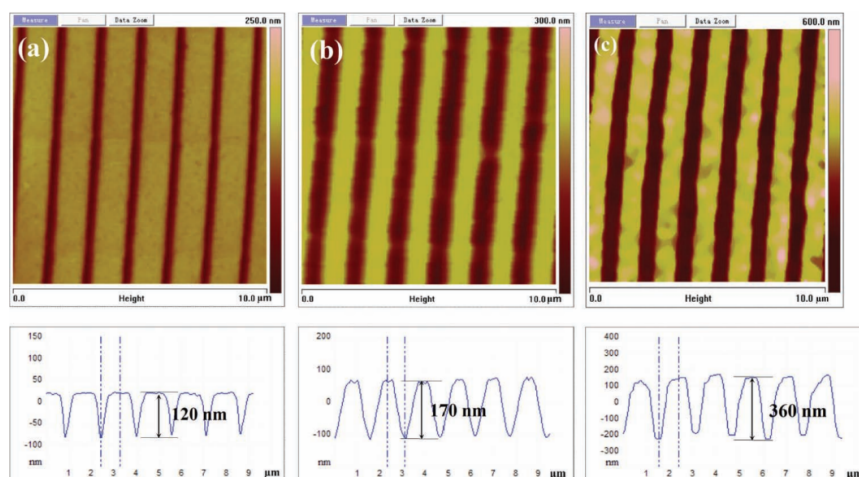


Figure 41 The perspective AFM and sectional-profile images of hybrid resist (a) imprinted, (b) after direct etching without transfer film and (c) after bilayer etching with PMMA as transfer film.^[136]

3.4. Hydrogel

Hydrogel, as a class of hydrophilic polymer with three-dimensional network, possesses the properties of absorbing and retaining a large amount of water due to many hydrophilic functional groups such as hydroxyl (-OH), carboxyl (-COOH), amino (-NH₂), sulfonic acid (-SO₃H) and so on, at the same time, maintaining their three-dimensional network structure.^[116, 137-141] Hydrogel materials are widely utilized in biomedical engineering and pharmaceutical industry due to biocompatibility, biodegradability, easy to synthesize and other merits.^[140-143]

At present, the formation methods of hydrogel mainly include physical and chemical crosslinking. The chemical crosslinking by means of forming chemical bond among monomer or oligomer is more stable than

physical crosslinking through weak interactions such as hydrogen bond.^[144] Chemical crosslinking includes Michael addition, Schiff base, enzymatic reaction, click chemistry, and photopolymerization.^[144] Among them, photopolymerization is probably the most effective and commonly crosslinking route. To form hydrogel by photopolymerization has many merits, firstly, the photopolymerization process is extremely rapid which could be completed in a few minutes or even seconds, secondly, the photopolymerization allows spatial and temporal control over the cross-linking process, this feature is particularly exploited by stereolithography and 3D-(bio)-printing, thirdly, there is no necessity for high temperature or extreme pH value because the photopolymerization process only requires lower energy and temperature.^[144-145] The mentioned-above technology has been specifically applied in the biological field.

For the last few years, as a 3D-(bio)-printing technology, Digital Light Processing (DLP) getting more and more attention because it can create more complex structure of tissue and organ.^[146-148] Hong et al.^[149] used the silk fibroin (SF) which modified by glycidyl methacrylate (GMA) to construct the chondrocyte-laden hydrogel scaffold using DLP 3D-printing technology by UV light source at 365 nm. The schematic diagram for modification of SF with GMA and bioprinting of chondrocyte with Silk-GMA DLP are illustrated in Figure 42. The Silk-GMA shows strong effectiveness for chondrogenesis *in vitro* and *in vivo* transplantation, meanwhile, suggests the good biocompatibilities and mechanical advantages for defected tissue regeneration.

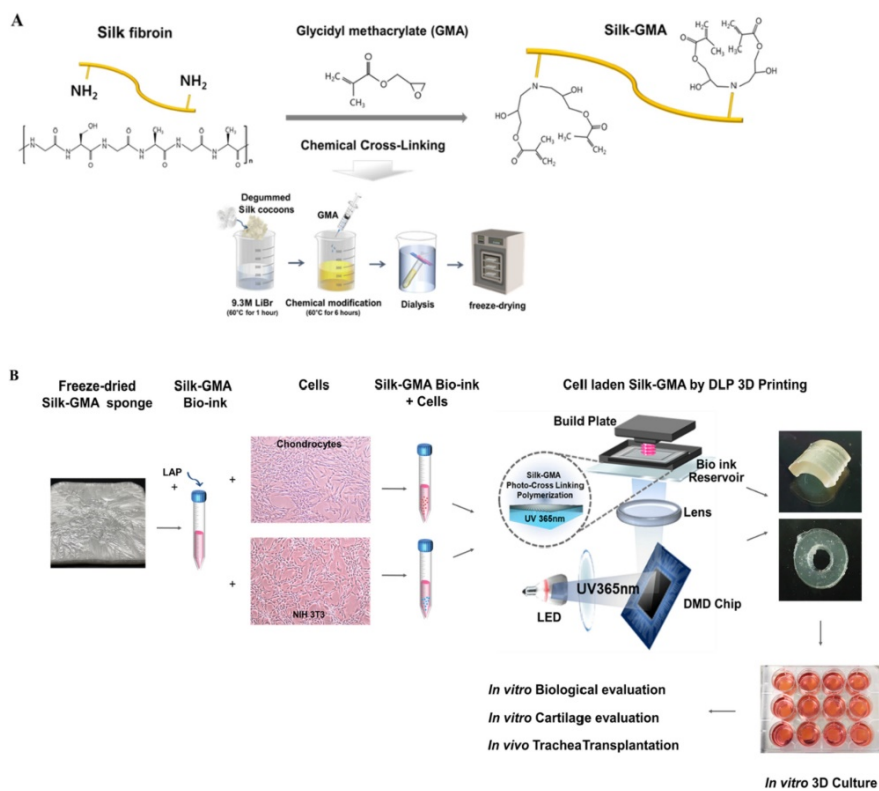


Figure 42 Schematic diagram for modification of SF with GMA (Silk-GMA) and bioprinting of chondrocyte with Silk-GMA DLP 3D-printing technology.^[149]

Gelatin methacryloyl (GelMA) has been utilized as precursor for 3D-printed hydrogels because its biological activity, fast photocrosslinking ability and temperature adjustable viscosity,^[150] whereas the poor mechanical strength, low stability and non-self-healing behavior have hampered its practical application in field of biomaterials. To deal with this limitation, Mao et al.^[151] synthesized a novel host-guest supramolecular compound HGSM which based on the inclusion interaction between cyclodextrin (CD) and adamantane (Ad), as exhibited in Figure 43. The HGSM that has three “arms” of acrylates and GelMA can photopolymerize to

construct the hydrogel HGGelMA which possesses the excellent mechanical and rapid self-healing properties due to the non-covalent bonds. Compared with pure GelMA hydrogel, the compression modulus of HGGelMA hydrogel increased by 525% which reached the level of most human soft tissues. In addition, the HGGelMA hydrogel displayed an excellent printability, The scaffold of 3D-printed HGGelMA hydrogel has the exquisite and homogeneous porous structures, good biocompatibility and histocompatibility with potential biomedical applications.

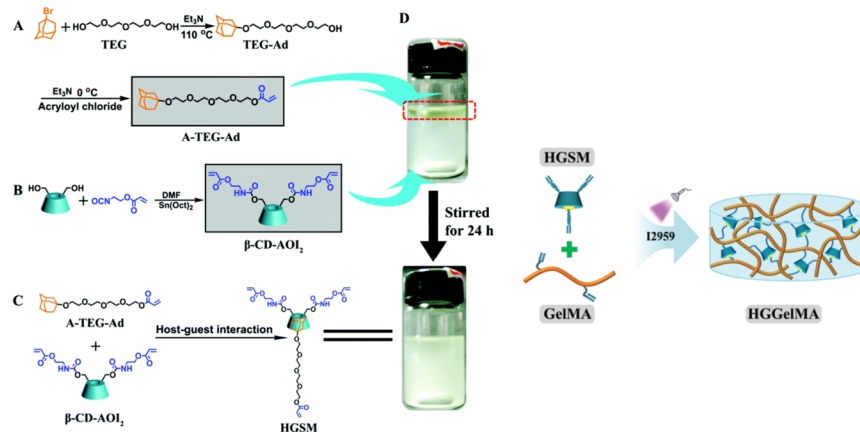


Figure 43 Schematic of the HGSM synthesis (left) and HGGelMA construction (right).^[151]

The water-soluble ultraviolet PI Irgacure 2959 has been widely used in cell encapsulation and tissue engineering,^[152-154] however, there are significant limitations to its application. Firstly, UV light has been known to be harmful for delivered cells and host tissues, secondly, its solubility in water is relatively poor.^[152, 155-156] Thus, the limitations of UV sources can be avoided by employing PI which could match to visible light. Lithium acylphosphinate salt (LAP) as a visible light PI possesses fine water solubility and allows cell encapsulation at lower PI concentrations, enabling efficient photopolymerization compared to Irgacure 2959. Monteiro et al.^[157] prepared the gelatin methacryloyl (GelMA) hydrogels encapsulating odontoblast-like cells by using dental curing devices (DL) with emission wavelength in visible light range, as shown in Figure 44. The results show that short-time exposure to DL did not significantly affect cell survival, simultaneously, preparation of GelMA hydrogels by DL source is faster than UV source, and showed higher cellular activity with larger pore sizes.

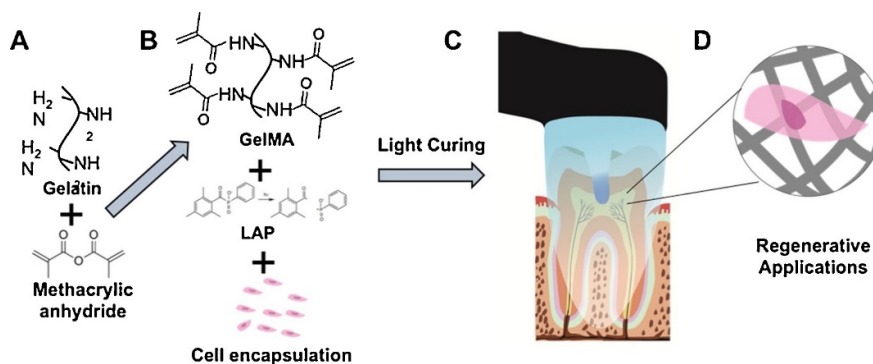


Figure 44 Synthesis of GelMA macromolecular monomers (A), cell encapsulation (B), process of photopolymerization (C) and cell-laden hydrogel materials (D).^[157]

In view of these advantages including high efficiency, safety, environmentally friendly and energy saving for visible light source, Shao et al.^[158] investigated the photopolymerization kinetics of the PIS which is composed of camphorquinone (CQ) and diphenyl iodonium hexafluorophosphate (DPI) that have been widely used as a blue light PIS. Then a hydrogel was synthesized by N, N-dimethylacrylamide (DMAA) and sodium acrylate (SA) according to the kinetic results. The CQ/DPI system resulted in fast polymerization and high double bond conversion (approximately 90 %) when maximum polymerization rate was approximately $6.53 \times 10^{-5} \text{ s}^{-1}$ with light intensity of 32.3 mW/cm^2 , 0.5 wt % CQ, and mass ratio of monomers was 4 (DMAA):6 (SA). The hydrogel synthesized by poly (DMAA/SA) under irradiation blue light displayed excellent water absorbability (about 750 g/g), robust mechanical properties (about 2500% strain and 0.6 MPa stress) and fine dimensional stability. The kinetic mechanisms proposed in this research can provide some reference for the synthesis of hydrogels in biomedical field.

Naphthalimide derivatives have been widely employed as PI in the field of visible light photopolymerization due to their excellent light absorption properties in visible light region. Lalevée et al.^[39, 159] synthesized a series of naphthalimide derivatives PIs that can be matched with LED sources with emission wavelengths of 385 nm, 405 nm, 455 nm and 470 nm, chemical structures of them are shown in Figure 45. The naphthalimide derivatives/additives systems can effectively initiate cationic radical polymerization, among them, NDP2 and 2,6-di-O-Me- β -cyclodextrin (DM- β -CD) can form supramolecular complex NPD2-CD together, which exhibited excellent solubility in water and good capacity of initiating polymerization of hydroxyethyl acrylate (HEA) to obtain hydrogel at exposure to 405 nm LED source, as shown in Figure 46.

Figure 45 Chemical structures of naphthalimide derivatives.

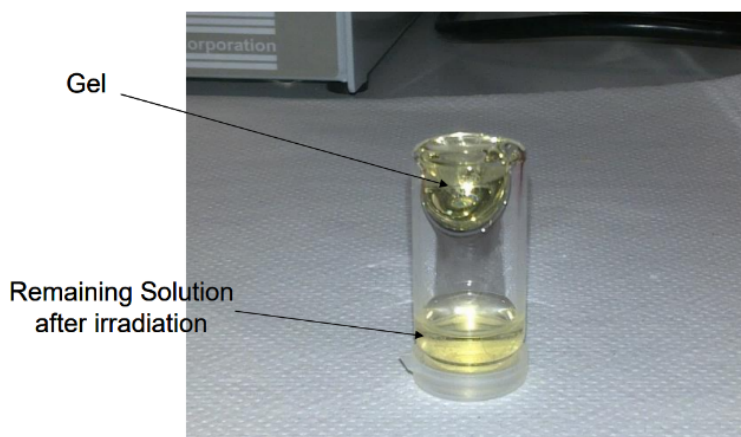


Figure 46 Preparation of poly (hydroxyethyl acrylate) in water by using NPD2-CD/MDEA system upon LED at 405nm irradiation.

The supramolecular complex DNND4/SBE- β -CD which was composed of DNND4 and sulfobutylether- β -cyclodextrin can also initiate polymerization reaction of HEA or hydroxyethyl methacrylate (HEMA) to obtain hydrogel under irradiation at 405 nm LED source.

The development of macromolecular water-soluble PIs with low-migration is extremely significant for achieving biosafety of photopolymerization. In terms of the preparation of hydrogels, Zhao et al.^[160] designed and synthesized a new lignin-based water-soluble macromolecular PI L-PEG-2959 based on the Irgacure 2959, in addition, the function of PEG chain in L-PEG-2959 is to improve the water solubility of lignin. Transparent hydrogel can be prepared by using glycidyl methacrylate modified gelatin as monomer and L-PEG-2959 as

PI. The synthesis of L-PEG-2959 and the preparation method of the hydrogel are displayed in Figure 47. Compared to the hydrogel containing Irgacure 2959, the extraction amount of L-PEG-2959 from the hydrogels was tremendously reduced, which indicates L-PEG-2959 is a promising macromolecular PI in fabricating biosafety hydrogel.

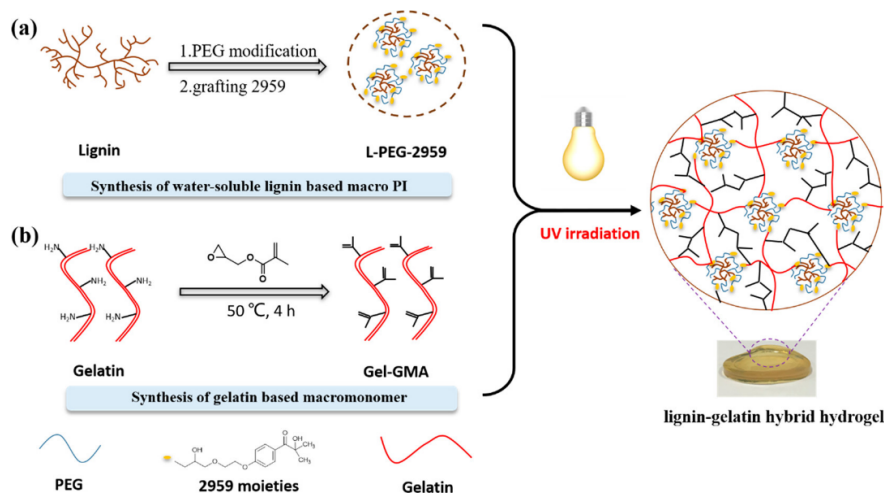


Figure 47 Fabrication process of lignin-gelatin hybrid hydrogel.

3.5. Applications of in photopolymerization other fields

In addition to the above fields, the application of photopolymerization is gradually expanding to other fields, such as frontal polymerization, photochromic materials, self-healing materials and so on.

Frontal polymerization is a self-propagating reaction where monomers are crosslinked into polymers by the propagation from localized reaction zone to entire system.^[161-162] Generally speaking, no extra energy is required except in initial stage.^[162] According to the initiation sources, frontal polymerization can be divided into the thermal-induced frontal polymerization (TFP) and photo-induced frontal polymerization (PFP).^[163] PFP is initiated by the irradiation usually UV light,^[164-166] however, as mentioned above, UV light has many disadvantages and limitations in practical application, it is a new strategy to use more secure NIR light as irradiation source of frontal polymerization. Based on this, our group employed a two-component system including cyanine (NIR sensitizer) and iodonium salt to initiate the frontal polymerization of cationic polymerizable monomers upon 808 nm NIR laser exposure.^[57] The heat released by NIR sensitizer and the polymerization reaction can dissociate AIBN or TPED to achieve frontal polymerization of vinyl ethers and epoxides. The frontal velocity and starting time can be modulate by changing the different kinds of monomers, thermal initiators and their concentration.

Solid-state photochromic materials especially photochromic polymers have potential application prospect in the fields of photoswitching devices, chemosensors, solid-state optical devices, imaging and 3D optical-data storage devices, and so on owing to their advantages of lightweight and good processability.^[167-171] At present, the main preparation method of photochromic polymers is thermopolymerization, which is complicated and energy consuming. Therefore, it is extremely meaningful to develop a simple, efficient and environmentally friendly preparation method of photochromic polymers.

Du et al.^[172] designed and synthesized two novel UV-LED-induced fluorophenyl oxime ester PIs (E-FBOXEs) with the ability to prepare photochromic polymers, and then photochromic polymers based on E-FBOXEs were prepared by fast photopolymerization. Proposed mechanism for the photochromism of the film initiated by E-FBOXEs is exhibited in Figure 48, Residual E-FBOXEs in photopolymerized films will generate

colored iminyl radicals in the planar conformation under irradiation at 395 nm, and the recombination of the radicals to form colorless E-FBOXEs in the nonplanar conformation under heating, which results in the photochromism of the polymeric films.

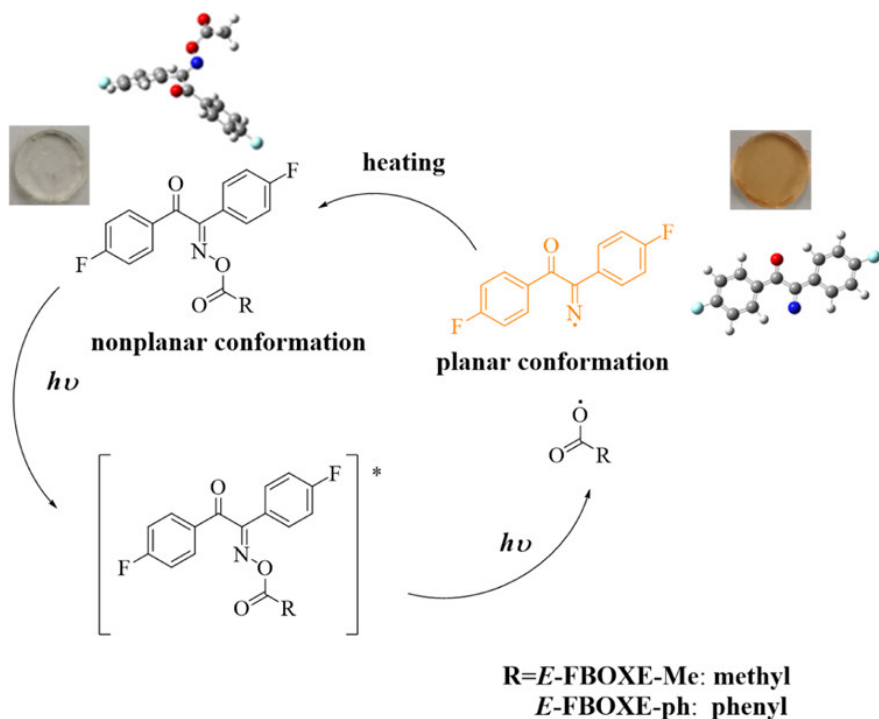


Figure 48 Proposed Photochromic Mechanism of E-FBOXEs.

The fast development of self-healing materials based on supramolecular interactions has attracted considerable attention in recent years,^[173-179] among the supramolecular interactions, ionic interactions are very interesting because of their high aggregation strength that results in low healing agent content for self-healing materials.^[180] However, most of self-healing materials based on ionic interactions are all thermocured materials.

Based on the above background, Sun et al.^[181] designed and synthesized a novel imidazolium-containing photocurable monomer, 6-(3-(3(2-hydroxyethyl)-1H-imidazol-3-ium bromide) propanoyloxy) hexyl acrylate (IM-A), based on 1,6-hexanediol diacrylate (HDDA) and 1H-imidazole and 2-bromoethanol, the synthesis route of IM-A is displayed in Figure 49. Then, the self-healing flexible materials was prepared by fast photocuring with IM-A, isobornyl acrylate (IBOA), 2-(2-ethoxyethoxy) ethyl acrylate (EOEOEA), and 2-hydroxyethyl acrylate (HEA). Herein, IM-A-containing imidazolium plays a self-healing role in the materials. The self-healing process of the photocured polymer contained IM-A is exhibited in Figure 50. The as-prepared self-healing polymer IB7-IM5 exhibited a tensile strength of 3.1 MPa, elongation at break of 205%, healing efficiency of 93%, and a wide healing temperature range from room temperature to 120 °C. The self-healing polymer was also employed as a flexible substrate to fabricate a flexible electronic device, which could be healed and completely restore its conductivity after the device was damaged.

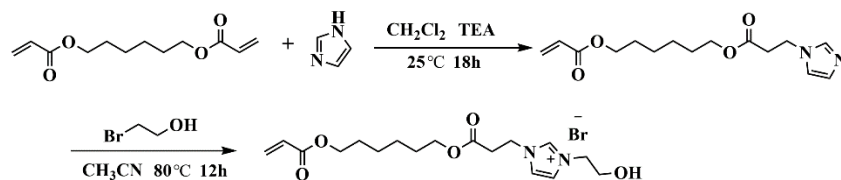


Figure 49 Synthesis route of IM-A.

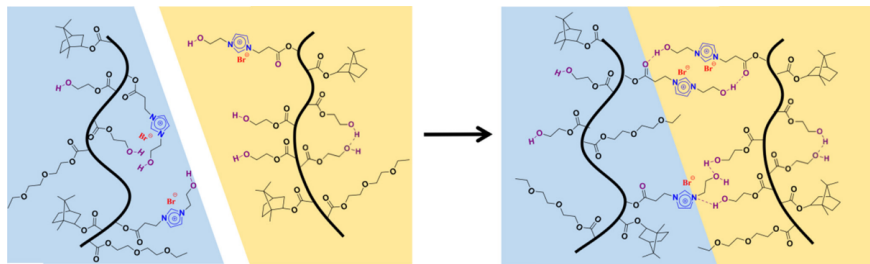


Figure 50 Illustration of the self-healing process of the photocured polymer.

Graphene quantum dots (GQDs) have important applications in photovoltaic devices, especially as emission layers in light-emitting diodes (leds) due to some merits such as outstanding photoluminescence properties, low toxicity, good biocompatibility, good electron transport capacity, and excellent thermal conductivity.^[182-186] However, GQDs usually suffer from serious fluorescence quenching in aggregates and the solid state due to easy agglomeration and aggregation-induced quenching, which seriously restrict their practical applications.^[187] For this reason, our group report a work which constructed the blue-emitting reduced graphene oxide quantum dot (rGOQD)-based light emitting diodes (LEDs) with efficient solid state emission by UV photolithography,^[188] as shown in Figure 51. In this work, preparing rGOQDs by the in situ photoreduction of graphene oxide quantum dot (GOQDs), preparation of the rGOQD/photoresist patterns, and the in situ photoreduction of GO in the aforementioned photoresist to rGO were achieved simultaneously. The PL spectrum for rGOQDs prepared by UV photolithography is observed to be blueshifted with a narrow FWHM compared to GOQDs, which leads to the fabrication of monochromatic blue-emitting devices.

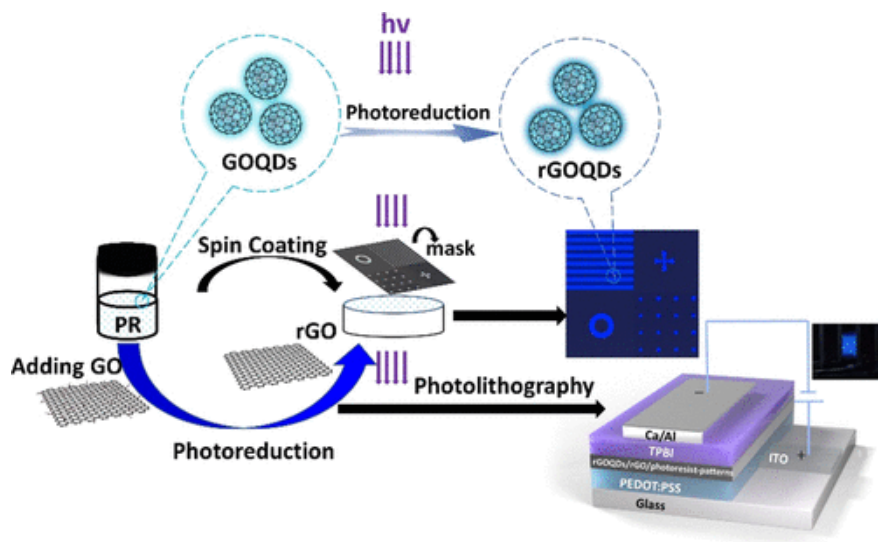


Figure 51 The preparation process of blue-emitting reduced graphene oxide quantum dot (rGOQD)-based light emitting diodes (LEDs).^[188]

Oxygen-containing functional groups of graphene oxide (GO), which destroy the path of electron movement, result in the conductivity of GO being far lower than that of graphene, which seriously restricts its application. Our group designed a kind of conductive patterned film with high resolution comprised of reduced graphene oxide (RGO) which prepared by the ultraviolet photolithography technique.^[189] This work developed a strategy of introducing GO into the photocuring formula and used UV photolithography technology to create conductive patterned polymer films in one step with high efficiency. BAPO not only acts as a PI to promote the photopolymerization of films under UV irradiation but also serves as a reductant to reduce GO. The mechanism for reducing GO in the composites by a simple and efficient photoreduction method is shown in Figure 52. Consequently, the maximum conductivity of photoresist/RGO films is 9.90 S cm^{-1} when the GO content is 10.7 wt%, BAPO content is 3 times that of GO and the exposure time is 15 min. Furthermore, conductive micropatterns can be obtained on diverse substrates such as PET films, silicon wafers and glasses substrates by photolithography techniques with a high conductivity of 0.98 S cm^{-1} , and the micropatterns demonstrate excellent flexibility and stability. This study suggests an approach to fabricate conductive polymer films and micropatterns with promising potential in the field of flexible electronic devices.

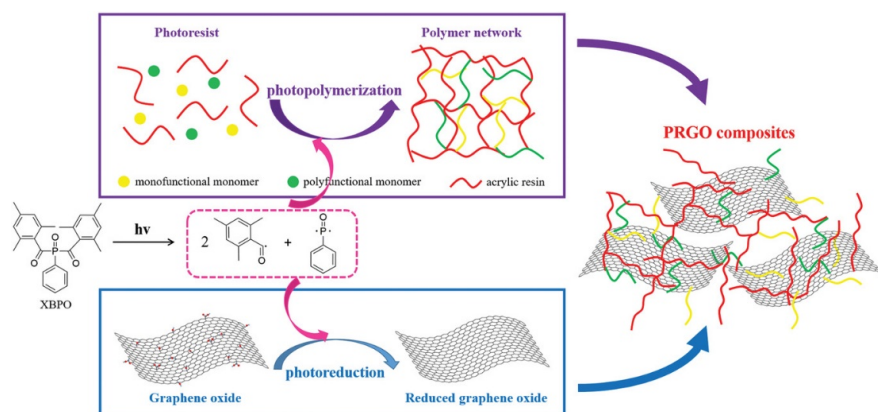


Figure 52 Schematic illustration of the formation of photoresist/RGO composites.^[189]

Summary and perspective

Due to the advantages of 5E (efficiency, enabling, economical, energy saving and environmental-friendly), photopolymerization technology has been applied in many fields, such as coatings, inks, adhesives, printing materials, microelectronic products, 3D printing, biological materials, etc., and plays an increasingly important role in our daily life. With the continuous development of technology and enhancement of environmental protection consciousness, photopolymerization will attract new development opportunities, simultaneously, it also faces new requirements. Firstly, it is a trend that LED photopolymerization replaces traditional UV photopolymerization. A large number of scientists are committed to the development of LED photopolymerization. So there are a lot of research results on LED photopolymerization in recent years. However, the color problem stemmed from the PIs also limits the application of LED photopolymerization in colorless and deep layer polymerization systems. In addition, the cost of producing LED source is relatively expensive, and further improvement of the manufacturing technology is needed. Secondly, the greenization of production process for photopolymerization raw material is also worth noting even though it as a green technology has been deeply rooted in people's concepts. Furthermore, the toxicity of PIs has attracted much attention, and many countries have introduced regulations or licensing lists to restrict the use of it. Therefore, it is very important to design PIs with low toxicity and high migration stability, or based on natural materials. Thirdly, radical photopolymerization will encounter some limitations in practical application due to its obviously shortcomings such as serious volume shrinkage and oxygen inhibition. For example, 3D printing based on radical photopolymerization system leads to the decrease of dimensional accuracy of products, while cationic photopolymerization can overcome the problem of volume shrinkage due to epoxy ring-opening. At present, the research of cationic photopolymerization needs further development to meet the application requirements. Last but not least, the development of new applications for photopolymerization technology is extremely necessary thing for its continuous progress, as well as the key factor that keeps it from being eliminated. For the moment, 3D printing, electronic information industry, biomaterials field, aviation field, etc. are the focus and research hotspots of the whole world scientific community. Researchers on photopolymerization technology should develop new applications to make photopolymerization continue to prosper.

AUTHOR INFORMATION

Corresponding Author

*E-mail: xinyangyang@mail.tsinghua.edu.cn (Yangyang Xin)

*E-mail: zouyq@bnu.edu.cn (Yingquan Zou)

ORCID

Xianglong He: 0000-0002-8352-463X

CONFLICTS OF INTEREST

The authors declare no competing financial interest.

ACKNOWLEDGMENT

The financial support from Hubei Gurun Technology Co., Ltd (10200-230210362) and Baoding Lucky Innovative Materials Co., Ltd (10200-230200095) is gratefully acknowledged.

REFERENCES

- [1] Z. Li, X. Zou, G. Zhu, X. Liu, R. Liu, *ACS Appl Mater Interfaces* **2018** , *10* , 16113-16123.
- [2] X. Ma, D. Cao, H. Fu, J. You, R. Gu, B. Fan, J. Nie, T. Wang, *Progress in Organic Coatings* **2019** , *135* , 517-524.

- [3] H. Pan, S. Chen, M. Jin, J.-P. Malval, D. Wan, F. Morlet-Savary, *Polymer Chemistry* **2019** , *10* , 1599-1609.
- [4] F. Xu, J.-L. Yang, Y.-S. Gong, G.-P. Ma, J. Nie, *Macromolecules* **2012** , *45* , 1158-1164.
- [5] C. Dietlin, T. T. Trinh, S. Schweizer, B. Graff, F. Morlet-Savary, P.-A. Noirot, J. Lalevée, *Macromolecules* **2019** , *52* , 7886-7893.
- [6] E. Hola, J. Ortyl, M. Jankowska, M. Pilch, M. Galek, F. Morlet-Savary, B. Graff, C. Dietlin, J. Lalevée, *Polymer Chemistry* **2020** , *11* , 922-935.
- [7] Z. Tang, Y. Gao, S. Jiang, J. Nie, F. Sun, *Progress in Organic Coatings* **2022** , *170* , 106969.
- [8] C. Dietlin, T. T. Trinh, S. Schweizer, B. Graff, F. Morlet-Savary, P. A. Noirot, J. Lalevee, *Molecules* **2020** , *25* .
- [9] M. Rahal, H. Bidotti, S. Duval, B. Graff, T. Hamieh, J. Toufaily, F. Dumur, J. Lalevée, *European Polymer Journal* **2022** , *177* , 111452.
- [10] F. Petko, M. Galek, E. Hola, R. Popielarz, J. Ortyl, *Macromolecules* **2021** , *54* , 7070-7087.
- [11] F. Hammoud, Z. H. Lee, B. Graff, A. Hijazi, J. Lalevée, Y. C. Chen, *Journal of Polymer Science* **2021** , *59* , 1711-1723.
- [12] J. Zhang, J. Lalevee, N. S. Hill, X. Peng, D. Zhu, J. Kiehl, F. Morlet-Savary, M. H. Stenzel, M. L. Coote, P. Xiao, *Macromol Rapid Commun* **2019** , *40* , e1900234.
- [13] J. V. Crivello, E. Reichmanis, *Chemistry of Materials* **2013** , *26* , 533-548.
- [14] V. Vijayakumar, B. Anothumakkool, S. Kurungot, M. Winter, J. R. Nair, *Energy & Environmental Science* **2021** , *14* , 2708-2788.
- [15] Y. Qi, X. Zhang, X. Huang, Y. Zhang, M. Shi, Y. Zhao, *Int J Biol Macromol* **2022** , *204* , 234-244.
- [16] W. Qiu, M. Li, Y. Yang, Z. Li, K. Dietliker, *Polymer Chemistry* **2020** , *11* , 1356-1363.
- [17] N. S. Hill, M. L. Coote, *Australian Journal of Chemistry* **2019** , *72* , 627.
- [18] C. Decker, *Polymer International* **2002** , *51* , 1141-1150.
- [19] B. B. Noble, A. C. Mater, L. M. Smith, M. L. Coote, *Polym. Chem.* **2016** , *7* , 6400-6412.
- [20] L.-J. Liu, W. Liu, G. Ji, Z.-Y. Wu, B. Xu, J. Qian, W.-J. Tian, *Chinese Journal of Polymer Science* **2019** , *37* , 401-408.
- [21] M. Nocita, A. Stevens, C. Noon, B. van Wesemael, *Geoderma* **2013** , *199* , 37-42.
- [22] E. G. Soltész, S. Kim, R. G. Laurence, A. M. DeGrand, C. P. Parungo, D. M. Dor, L. H. Cohn, M. G. Bawendi, J. V. Frangioni, T. Mihaljevic, *Ann Thorac Surg* **2005** , *79* , 269-277; discussion 269-277.
- [23] J. Yu, Y. Gao, S. Jiang, F. Sun, *Macromolecules* **2019** , *52* , 1707-1717.
- [24] C. Xie, Z. Wang, Y. Liu, L. Song, L. Liu, Z. Wang, Q. Yu, *Progress in Organic Coatings* **2019** , *135* , 34-40.
- [25] E. Frick, C. Schweigert, B. B. Noble, H. A. Ernst, A. Lauer, Y. Liang, D. Voll, M. L. Coote, A.-N. Unterreiner, C. Barner-Kowollik, *Macromolecules* **2015** , *49* , 80-89.
- [26] X. Ma, R. Gu, L. Yu, W. Han, J. Li, X. Li, T. Wang, *Polymer Chemistry* **2017** , *8* , 6134-6142.
- [27] J. Zhou, X. Allonas, A. Ibrahim, X. Liu, *Progress in Polymer Science* **2019** , *99* , 101165.
- [28] P. Gauss, M. Griesser, M. Markovic, A. Ovsianikov, G. Gescheidt, P. Knaack, R. Liska, *Macromolecules* **2019** , *52* , 2814-2821.

- [29] X. Ju, X. Hu, Y. Gao, J. Nie, F. Sun, *Progress in Organic Coatings* **2022** , 162 , 106562.
- [30] X. He, Y. Gao, J. Nie, F. Sun, *Macromolecules* **2021** , 54 , 3854-3864.
- [31] M. Bouzrati-Zerelli, J. Kirschner, C. P. Fik, M. Maier, C. Dietlin, F. Morlet-Savary, J. P. Fouassier, J.-M. Becht, J. E. Klee, J. Lalevée, *Macromolecules* **2017** , 50 , 6911-6923.
- [32] S. Chen, M. Jin, J.-P. Malval, J. Fu, F. Morlet-Savary, H. Pan, D. Wan, *Polymer Chemistry* **2019** , 10 , 6609-6621.
- [33] W. Han, H. Fu, T. Xue, T. Liu, Y. Wang, T. Wang, *Polymer Chemistry* **2018** , 9 , 1787-1798.
- [34] N. Karaca, N. Ocal, N. Arsu, S. Jockusch, *Journal of Photochemistry and Photobiology A: Chemistry* **2016** , 331 , 22-28.
- [35] J. Zhang, K. Launay, N. S. Hill, D. Zhu, N. Cox, J. Langley, J. Lalevée, M. H. Stenzel, M. L. Coote, P. Xiao, *Macromolecules* **2018** , 51 , 10104-10112.
- [36] J. Zhang, J. Lalevée, N. S. Hill, K. Launay, F. Morlet-Savary, B. Graff, M. H. Stenzel, M. L. Coote, P. Xiao, *Macromolecules* **2018** , 51 , 8165-8173.
- [37] K. Sun, Y. Xu, F. Dumur, F. Morlet-Savary, H. Chen, C. Dietlin, B. Graff, J. Lalevée, P. Xiao, *Polymer Chemistry* **2020** , 11 , 2230-2242.
- [38] S. Liu, D. Brunel, K. Sun, Y. Xu, F. Morlet-Savary, B. Graff, P. Xiao, F. Dumur, J. Lalevée, *Polymer Chemistry* **2020** , 11 , 3551-3556.
- [39] J. Zhang, F. Dumur, P. Xiao, B. Graff, D. Bardelang, D. Gignes, J. P. Fouassier, J. Lalevée, *Macromolecules* **2015** , 48 , 2054-2063.
- [40] A. Al Mousawi, A. Arar, M. Ibrahim-Ouali, S. Duval, F. Dumur, P. Garra, J. Toufaily, T. Hamieh, B. Graff, D. Gignes, J. P. Fouassier, J. Lalevee, *Photochem Photobiol Sci* **2018** , 17 , 578-585.
- [41] J. Zhang, M. Frigoli, F. Dumur, P. Xiao, L. Ronchi, B. Graff, F. Morlet-Savary, J. P. Fouassier, D. Gignes, J. Lalevée, *Macromolecules* **2014** , 47 , 2811-2819.
- [42] M. Abdallah, T.-T. Bui, F. Goubard, D. Theodosopoulou, F. Dumur, A. Hijazi, J.-P. Fouassier, J. Lalevée, *Polymer Chemistry* **2019** , 10 , 6145-6156.
- [43] S. Fan, X. Sun, X. He, Y. Pang, Y. Xin, Y. Ding, Y. Zou, *Polymers (Basel)* **2022** , 14 .
- [44] J. Kirschner, A. Baralle, B. Graff, J. M. Becht, J. E. Klee, J. Lalevee, *Macromol Rapid Commun* **2019** , 40 , e1900319.
- [45] J. Kirschner, J. Paillard, B. Graff, J. M. Becht, J. E. Klee, J. Lalevée, *Macromolecular Chemistry and Physics* **2020** , 221 , 1900495.
- [46] B. Ganster, U. K. Fischer, N. Moszner, R. Liska, *Macromolecular Rapid Communications* **2008** , 29 , 57-62.
- [47] A. Eibel, D. E. Fast, G. Gescheidt, *Polymer Chemistry* **2018** , 9 , 5107-5115.
- [48] B. Ganster, U. K. Fischer, N. Moszner, R. Liska, *Macromolecules* **2008** , 41 , 2394-2400.
- [49] P. Xiao, F. Dumur, B. Graff, J. P. Fouassier, D. Gignes, J. Lalevée, *Macromolecules* **2013** , 46 , 6744-6750.
- [50] J. Li, Y. Hao, M. Zhong, L. Tang, J. Nie, X. Zhu, *Dyes and Pigments* **2019** , 165 , 467-473.
- [51] A. Al Mousawi, C. Poriel, F. Dumur, J. Toufaily, T. Hamieh, J. P. Fouassier, J. Lalevée, *Macromolecules* **2017** , 50 , 746-753.

- [52] G. Noirbent, Y. Xu, A.-H. Bonardi, D. Gigmes, J. Lalevée, F. Dumur, *European Polymer Journal* **2020** , *139* , 110019.
- [53] A. H. Bonardi, F. Dumur, T. M. Grant, G. Noirbent, D. Gigmes, B. H. Lessard, J. P. Fouassier, J. Lalevée, *Macromolecules***2018** , *51* , 1314-1324.
- [54] Y. Pang, A. Shiraishi, D. Keil, S. Popov, V. Strehmel, H. Jiao, J. S. Gutmann, Y. Zou, B. Strehmel, *Angew Chem Int Ed Engl***2021** , *60* , 1465-1473.
- [55] B. Strehmel, C. Schmitz, C. Kutahya, Y. Pang, A. Drewitz, H. Mustroph, *Beilstein J Org Chem* **2020** , *16* , 415-444.
- [56] C. Schmitz, A. Halbhuber, D. Keil, B. Strehmel, *Progress in Organic Coatings* **2016** , *100* , 32-46.
- [57] Y. Xin, S. Xiao, Y. Pang, Y. Zou, *Progress in Organic Coatings* **2021** , *153* , 106149.
- [58] Y. Pang, S. Fan, Q. Wang, D. Oprych, A. Feilen, K. Reiner, D. Keil, Y. L. Slominsky, S. Popov, Y. Zou, B. Strehmel, *Angew Chem Int Ed Engl* **2020** , *59* , 11440-11447.
- [59] D. Oprych, C. Schmitz, C. Ley, X. Allonas, E. Ermilov, R. Erdmann, B. Strehmel, *ChemPhotoChem* **2019** , *3* , 1119-1126.
- [60] S. Wu, H. J. Butt, *Adv Mater* **2016** , *28* , 1208-1226.
- [61] T. Brömme, C. Schmitz, D. Oprych, A. Wenda, V. Strehmel, M. Grabolle, U. Resch-Genger, S. Ernst, K. Reiner, D. Keil, P. Lüs, H. Baumann, B. Strehmel, *Chemical Engineering & Technology***2016** , *39* , 13-25.
- [62] C. Schmitz, B. Strehmel, *ChemPhotoChem* **2017** , *1* , 26-34.
- [63] J. Zhu, Q. Zhang, T. Yang, Y. Liu, R. Liu, *Nat Commun***2020** , *11* , 3462.
- [64] C. E. Hoyle, C. N. Bowman, *Angew Chem Int Ed Engl***2010** , *49* , 1540-1573.
- [65] P. Esfandiari, S. C. Ligon, J. J. Lagref, R. Frantz, Z. Cherkaoui, R. Liska, *Journal of Polymer Science Part A: Polymer Chemistry* **2013** , *51* , 4261-4266.
- [66] T. O. Machado, C. Sayer, P. H. H. Araujo, *European Polymer Journal* **2017** , *86* , 200-215.
- [67] J. Zhou, Q.-y. Zhang, S.-j. Chen, H.-p. Zhang, A.-j. Ma, M.-l. Ma, Q. Liu, J.-j. Tan, *Polymer Testing* **2013** , *32* , 608-616.
- [68] Z. Yang, Y. Bai, B. Wei, Y. Cui, J. Huang, Y. Li, L. Meng, Y. Wang, *Progress in Organic Coatings* **2023** , *174* , 107248.
- [69] H. C. Kolb, M. G. Finn, K. B. Sharpless, *Angewandte Chemie International Edition* **2001** , *40* , 2004-2021.
- [70] Z. Lin, Y. Ke, X. Peng, X. Wu, C. Zhang, H. Zhao, P. Feng, *ACS Applied Polymer Materials* **2022** , *4* , 5330-5340.
- [71] N. Z. Fantoni, A. H. El-Sagheer, T. Brown, *Chem Rev***2021** , *121* , 7122-7154.
- [72] B. D. Fairbanks, L. J. Macdougall, S. Mavila, J. Sinha, B. E. Kirkpatrick, K. S. Anseth, C. N. Bowman, *Chem Rev* **2021** , *121* , 6915-6990.
- [73] E. Blasco, M. Wegener, C. Barner-Kowollik, *Adv Mater***2017** , *29* .
- [74] W. Guo, Y. Jia, K. Tian, Z. Xu, J. Jiao, R. Li, Y. Wu, L. Cao, H. Wang, *ACS Appl Mater Interfaces* **2016** , *8* , 21046-21054.
- [75] Y. Su, S. Zhang, X. Zhou, Z. Yang, T. Yuan, *Progress in Organic Coatings* **2020** , *148* , 105880.
- [76] Y. Su, H. Lin, S. Zhang, Z. Yang, T. Yuan, *Polymers (Basel)* **2020** , *12* .

- [77] Z. Chu, Y. Feng, B. Xie, Y. Yang, Y. Hu, X. Zhou, T. Yuan, Z. Yang, *Industrial Crops and Products* **2021** , 160 , 113117.
- [78] S. Molina-Gutierrez, A. Manseri, V. Ladmiral, R. Bongiovanni, S. Caillol, P. Lacroix-Desmazes, *Macromolecular Chemistry and Physics* **2019** , 220 , 1900179.
- [79] Q. Wang, H. Cui, X. Wang, Z. Hu, P. Tao, M. Li, J. Wang, Y. Tang, H. Xu, X. He, *J Am Chem Soc* **2023** , 145 , 3064-3074.
- [80] A. Bagheri, J. Jin, *ACS Applied Polymer Materials* **2019** , 1 , 593-611.
- [81] J. U. Pucci, B. R. Christophe, J. A. Sisti, E. S. Connolly, Jr., *Biotechnol Adv* **2017** , 35 , 521-529.
- [82] Z. Rahman, S. F. Barakh Ali, T. Ozkan, N. A. Charoo, I. K. Reddy, M. A. Khan, *AAPS J* **2018** , 20 , 101.
- [83] L. M. Stevens, C. Tagnon, Z. A. Page, *ACS Appl Mater Interfaces* **2022** .
- [84] Y. Bao, *Macromol Rapid Commun* **2022** , 43 , e2200202.
- [85] X. Xu, P. Robles-Martinez, C. M. Madla, F. Joubert, A. Goyanes, A. W. Basit, S. Gaisford, *Additive Manufacturing* **2020** , 33 , 101071.
- [86] M. Belqat, X. Wu, J. Morris, K. Mougin, T. Petithory, L. Pieuchot, Y. Guillaneuf, D. Gignes, J. L. Clement, A. Spangenberg, *Advanced Functional Materials* **2023** , 2211971.
- [87] G. Zhu, J. Zhang, J. Huang, Y. Qiu, M. Liu, J. Yu, C. Liu, Q. Shang, Y. Hu, L. Hu, Y. Zhou, *Chemical Engineering Journal* **2023** , 452 , 139401.
- [88] V. Vlnieska, E. Gilshtein, D. Kunka, J. Heier, Y. E. Romanyuk, *Polymers (Basel)* **2022** , 14 .
- [89] J. Zhu, Z. Guo, Y. Zhou, X. Zou, Y. Zhu, Y. Liu, R. Liu, *Advanced Materials Technologies* **2023** , 2201613.
- [90] D. Zhu, X. Peng, P. Xiao, *Additive Manufacturing* **2022** , 59 , 103154.
- [91] S. C. Ligon, R. Liska, J. Stampfl, M. Gurr, R. Mulhaupt, *Chem Rev* **2017** , 117 , 10212-10290.
- [92] N. D. Dolinski, Z. A. Page, E. B. Callaway, F. Eisenreich, R. V. Garcia, R. Chavez, D. P. Bothman, S. Hecht, F. W. Zok, C. J. Hawker, *Adv Mater* **2018** , 30 , e1800364.
- [93] X. Zhao, Y. Zhao, M. D. Li, Z. Li, H. Peng, T. Xie, X. Xie, *Nat Commun* **2021** , 12 , 2873.
- [94] P. Xiao, J. Zhang, F. Dumur, M. A. Tehfe, F. Morlet-Savary, B. Graff, D. Gignes, J. P. Fouassier, J. Lalevee, *Progress in Polymer Science* **2015** , 41 , 32-66.
- [95] P. Lederhose, Z. Chen, R. Muller, J. P. Blinco, S. Wu, C. Barner-Kowollik, *Angew Chem Int Ed Engl* **2016** , 55 , 12195-12199.
- [96] S. Wu, J. P. Blinco, C. Barner-Kowollik, *Chemistry* **2017** , 23 , 8325-8332.
- [97] C. Luo, C. Xu, L. Lv, H. Li, X. Huang, W. Liu, *RSC Advances* **2020** , 10 , 8385-8395.
- [98] D. Suwandi, R. Aziz, A. Sifa, E. Haris, J. Istiyanto, Y. Whulanza, *International Journal of Technology* **2019** , 10 , 1033.
- [99] H. S. Lee, H. H. Yang, S. Ra, J. B. Yoon, *Journal of Micromechanics and Microengineering* **2011** , 21 , 065026.
- [100] S. Suzuki, J. Iwaki, T. Urano, S. Takahara, T. Yamaoka, *Polymers for Advanced Technologies* **2006** , 17 , 348-353.
- [101] S. Myeong, B. Chon, S. Kumar, H. J. Son, S. O. Kang, S. Seo, *Nanoscale Adv* **2022** , 4 , 1080-1087.

- [102] H.-Y. Lin, C.-W. Sher, D.-H. Hsieh, X.-Y. Chen, H.-M. P. Chen, T.-M. Chen, K.-M. Lau, C.-H. Chen, C.-C. Lin, H.-C. Kuo, *Photonics Research* **2017** , 5 , 411.
- [103] P. Li, X. Zhang, Y. Li, L. Qi, C. W. Tang, K. M. Lau, *Journal of the Society for Information Display* **2020** ,29 , 157-165.
- [104] M.-H. Chen, C.-C. Lai, H.-L. Chen, Y.-H. Lin, K.-Y. Huang, C.-H. Lin, H.-T. Hsiao, L.-C. Liu, C.-M. Chen, *Materials Science in Semiconductor Processing* **2018** , 88 , 132-138.
- [105] P. Mukherjee, F. Nebuloni, H. Gao, J. Zhou, I. Papautsky, *Micromachines (Basel)* **2019** , 10 .
- [106] S. Farjana, M. Ghaderi, S. Rahiminejad, S. Haasl, P. Enoksson, *Micromachines (Basel)* **2021** , 12 .
- [107] Y. C. Tsai, H. P. Jen, K. W. Lin, Y. Z. Hsieh, *J Chromatogr A* **2006** , 1111 , 267-271.
- [108] R. Bruch, A. Kling, G. A. Urban, C. Dincer, *J Vis Exp* **2017** .
- [109] Y. Ding, Y. Xin, Q. Zhang, Y. Zou, *Materials & Design* **2022** , 213 , 110370.
- [110] H. Y. Huang, H. Chen, *Molecular Crystals and Liquid Crystals* **2011** , 548 , 3-16.
- [111] H. Sugita, N. Matsumura, *Microelectronic Engineering* **2018** , 195 , 86-94.
- [112] Y. C. Chen, Y. T. Kuo, T. H. Ho, *Photochem Photobiol Sci* **2019** , 18 , 190-197.
- [113] X. Jiang, J. Yin, Y. Murakami, M. Kaji, *J Photopolym Sci Tec* **2009** , 22 , 351-356.
- [114] J. Lei, T. Akitoshi, S. Katou, Y. Murakami, J. Yin, X. Jiang, *Macromolecular Chemistry and Physics* **2019** , 220 , 1900152.
- [115] E. Hola, M. Topa, A. Chachaj-Brekiesz, M. Pilch, P. Fiedor, M. Galek, J. Ortyl, *RSC Adv* **2020** , 10 , 7509-7522.
- [116] A. Borchers, T. Pieler, *Genes (Basel)* **2010** ,1 , 413-426.
- [117] M. Sangermano, A. Di Gianni, G. Malucelli, C. Roncuzzi, A. Priola, B. Voit, *Journal of Applied Polymer Science* **2005** , 97 , 293-299.
- [118] J. V. Crivello, *Journal of Polymer Science Part A: Polymer Chemistry* **2015** , 53 , 594-601.
- [119] J. Lee, K.-H. Choi, K. Yoo, *Micromachines* **2014** , 6 , 1-18.
- [120] G. Blagoi, S. Keller, A. Johansson, A. Boisen, M. Dufva, *Applied Surface Science* **2008** , 255 , 2896-2902.
- [121] X. Zhang, L. Du, Z. Xu, *Journal of Applied Polymer Science* **2013** , 127 , 4456-4462.
- [122] C. R. A. Lima, J. Silva Martins, C. Pinheiro, L. F. Avila, R. R. Pinho, M. L. M. Rocco, W. Souza Melo, F. Zappa, *Journal of Polymer Science Part B: Polymer Physics* **2019** .
- [123] B. Nowduri, S. Schulte, D. Decker, K. H. Schafer, M. Saumer, *Advanced Functional Materials* **2020** , 30 , 2004227.
- [124] M. C. Traub, W. Longsine, V. N. Truskett, *Annu Rev Chem Biomol Eng* **2016** , 7 , 583-604.
- [125] M. Zhang, S. Jiang, Y. Gao, J. Nie, F. Sun, *Chemical Engineering Journal* **2020** , 390 , 124625.
- [126] C. Zhang, H. Subbaraman, Q. Li, Z. Pan, J. G. Ok, T. Ling, C.-J. Chung, X. Zhang, X. Lin, R. T. Chen, L. J. Guo, *Journal of Materials Chemistry C* **2016** , 4 , 5133-5153.
- [127] Y. Ofir, I. W. Moran, C. Subramani, K. R. Carter, V. M. Rotello, *Adv Mater* **2010** , 22 , 3608-3614.
- [128] T. Ngai, C. Wu, *Macromolecules* **2003** , 36 , 848-854.
- [129] H. Lin, X. Wan, Z. Li, X. Jiang, Q. Wang, J. Yin, *ACS Applied Materials & Interfaces* **2010** , 2 , 2076-2082.

- [130] C. Zhao, C. Shao, X. Yu, D. Yang, J. Wei, *The Journal of Physical Chemistry C* **2017** , *121* , 11428-11436.
- [131] D. Matsukawa, H. Okamura, M. Shirai, *Journal of Materials Chemistry* **2011** , *21* , 10407.
- [132] M. Zhang, S. Jiang, Y. Gao, J. Nie, F. Sun, *Industrial & Engineering Chemistry Research* **2020** , *59* , 7564-7574.
- [133] E. Tegou, *Microelectronic Engineering* **2004** , *73-74* , 238-243.
- [134] G. M. Schmid, M. D. Stewart, J. Wetzel, F. Palmieri, J. Hao, Y. Nishimura, K. Jen, E. K. Kim, D. J. Resnick, J. A. Liddle, C. G. Willson, *Journal of Vacuum Science & Technology B: Microelectronics and Nanometer Structures* **2006** , *24* , 1283.
- [135] B. K. Lee, N. G. Cha, L. Y. Hong, D. P. Kim, H. Tanaka, H. Y. Lee, T. Kawai, *Langmuir* **2010** , *26* , 14915-14922.
- [136] H. Lin, X. Wan, X. Jiang, Q. Wang, J. Yin, *Advanced Functional Materials* **2011** , *21* , 2960-2967.
- [137] Y. Li, H. Wang, Y. Niu, S. Ma, Z. Xue, A. Song, S. Zhang, W. Xu, C. Ren, *ChemistrySelect* **2019** , *4* , 14036-14042.
- [138] C. Xing, S. Chen, X. Liang, Q. Liu, M. Qu, Q. Zou, J. Li, H. Tan, L. Liu, D. Fan, H. Zhang, *ACS Appl Mater Interfaces* **2018** , *10* , 27631-27643.
- [139] Y. Zheng, Y. Xie, A. Wang, *Chemical Engineering Journal* **2012** , *179* , 90-98.
- [140] G. Sharma, B. Thakur, M. Naushad, A. Kumar, F. J. Stadler, S. M. Alfadul, G. T. Mola, *Environmental Chemistry Letters* **2017** , *16* , 113-146.
- [141] M. C. Catoira, L. Fusaro, D. Di Francesco, M. Ramella, F. Boccafosci, *J Mater Sci Mater Med* **2019** , *30* , 115.
- [142] S. Ahmad, M. Ahmad, K. Manzoor, R. Purwar, S. Ikram, *Int J Biol Macromol* **2019** , *136* , 870-890.
- [143] Z. Bao, C. Xian, Q. Yuan, G. Liu, J. Wu, *Adv Healthc Mater* **2019** , *8* , e1900670.
- [144] A. Sun, X. He, X. Ji, D. Hu, M. Pan, L. Zhang, Z. Qian, *Chinese Chemical Letters* **2021** , *32* , 2117-2126.
- [145] E. Nicol, *Biomacromolecules* **2021** , *22* , 1325-1345.
- [146] M. Zhou, W. Liu, H. Wu, X. Song, Y. Chen, L. Cheng, F. He, S. Chen, S. Wu, *Ceramics International* **2016** , *42* , 11598-11602.
- [147] C. A. Mandon, L. J. Blum, C. A. Marquette, *Analytical Chemistry* **2016** , *88* , 10767-10772.
- [148] W. Zhu, X. Ma, M. Gou, D. Mei, K. Zhang, S. Chen, *Curr Opin Biotechnol* **2016** , *40* , 103-112.
- [149] H. Hong, Y. B. Seo, D. Y. Kim, J. S. Lee, Y. J. Lee, H. Lee, O. Ajiteru, M. T. Sultan, O. J. Lee, S. H. Kim, C. H. Park, *Biomaterials* **2020** , *232* , 119679.
- [150] A. I. Neto, P. A. Levkin, J. F. Mano, *Materials Horizons* **2018** , *5* , 379-393.
- [151] Z. Wang, G. An, Y. Zhu, X. Liu, Y. Chen, H. Wu, Y. Wang, X. Shi, C. Mao, *Mater Horiz* **2019** , *6* , 733-742.
- [152] B. D. Fairbanks, M. P. Schwartz, C. N. Bowman, K. S. Anseth, *Biomaterials* **2009** , *30* , 6702-6707.
- [153] C. G. Williams, A. N. Malik, T. K. Kim, P. N. Manson, J. H. Elisseeff, *Biomaterials* **2005** , *26* , 1211-1218.
- [154] N. E. Fedorovich, M. H. Oudshoorn, D. van Geemen, W. E. Hennink, J. Alblas, W. J. A. Dhert, *Biomaterials* **2009** , *30* , 344-353.

- [155] N. Annabi, A. Tamayol, J. A. Uquillas, M. Akbari, L. E. Bertassoni, C. Cha, G. Camci-Unal, M. R. Dokmeci, N. A. Peppas, A. Khademhosseini, *Adv Mater* **2014** , *26* , 85-123.
- [156] U. P. Kappes, D. Luo, M. Potter, K. Schulmeister, T. M. Runger, *J Invest Dermatol* **2006** , *126* , 667-675.
- [157] N. Monteiro, G. Thirivikraman, A. Athirasala, A. Tahayeri, C. M. Franca, J. L. Ferracane, L. E. Bertassoni, *Dent Mater* **2018** , *34* , 389-399.
- [158] G. Sun, Y. Huang, D. Li, E. Chen, Y. Zhong, Q. Fan, J. Shao, *Industrial & Engineering Chemistry Research* **2019** , *58* , 9266-9275.
- [159] N. Zivic, J. Zhang, D. Bardelang, F. Dumur, P. Xiao, T. Jet, D.-L. Versace, C. Dietlin, F. Morlet-Savary, B. Graff, J. P. Fouassier, D. Gimes, J. Lalevee, *Polymer Chemistry* **2016** , *7* , 418-429.
- [160] Y. Liu, X. Huang, K. Han, Y. Dai, X. Zhang, Y. Zhao, *ACS Sustainable Chemistry & Engineering* **2019** , *7* , 4004-4011.
- [161] A. Kumar, Y. Gao, P. H. Geubelle, *Journal of Polymer Science* **2021** , *59* , 1109-1118.
- [162] I. D. Robertson, H. L. Hernandez, S. R. White, J. S. Moore, *ACS Appl Mater Interfaces* **2014** , *6* , 18469-18474.
- [163] Q. Li, H.-X. Shen, C. Liu, C.-F. Wang, L. Zhu, S. Chen, *Progress in Polymer Science* **2022** , *127* , 101514.
- [164] J. T. Cabral, J. F. Douglas, *Polymer* **2005** , *46* , 4230-4241.
- [165] J. V. Crivello, *Polymer* **2005** , *46* , 12109-12117.
- [166] Y. Cui, J. Yang, Z. Zeng, Z. Zeng, Y. Chen, *Polymer* **2007** , *48* , 5994-6001.
- [167] N. Begum, S. Kaur, Y. Xiang, H. Yin, G. Mohiuddin, N. V. S. Rao, S. K. Pal, *The Journal of Physical Chemistry C* **2019** , *124* , 874-885.
- [168] L. Qu, X. Xu, J. Song, D. Wu, L. Wang, W. Zhou, X. Zhou, H. Xiang, *Dyes and Pigments* **2020** , *181* , 108597.
- [169] C. Li, K. Xiong, Y. Chen, C. Fan, Y. L. Wang, H. Ye, M. Q. Zhu, *ACS Appl Mater Interfaces* **2020** , *12* , 27651-27662.
- [170] J. Jiang, P. Zhang, L. Liu, Y. Li, Y. Zhang, T. Wu, H. Xie, C. Zhang, J. Cui, J. Chen, *Chemical Engineering Journal* **2021** , *425* , 131557.
- [171] L. Wang, W. Xiong, H. Tang, D. Cao, *Journal of Materials Chemistry C* **2019** , *7* , 9102-9111.
- [172] Y. Ding, S. Jiang, Y. Gao, J. Nie, H. Du, F. Sun, *Macromolecules* **2020** , *53* , 5701-5710.
- [173] L. R. Hart, N. A. Nguyen, J. L. Harries, M. E. Mackay, H. M. Colquhoun, W. Hayes, *Polymer* **2015** , *69* , 293-300.
- [174] Y. Chen, W. Wu, T. Himmel, M. H. Wagner, *Macromolecular Materials and Engineering* **2013** , *298* , 876-887.
- [175] C.-C. Cheng, F.-C. Chang, J.-K. Chen, T.-Y. Wang, D.-J. Lee, *RSC Advances* **2015** , *5* , 101148-101154.
- [176] M. Enke, D. Dohler, S. Bode, W. H. Binder, M. D. Hager, U. S. Schubert, **2015** , *273* , 59-112.
- [177] G. Sinawang, M. Osaki, Y. Takashima, H. Yamaguchi, A. Harada, *Chem Commun (Camb)* **2020** , *56* , 4381-4395.
- [178] M. Mohamadhoseini, Z. Mohamadnia, *Coordination Chemistry Reviews* **2021** , *432* , 213711.

- [179] J. Xie, P. Yu, Z. Wang, J. Li, *Biomacromolecules* **2022** , *23* , 641-660.
- [180] N. K. James, U. Lafont, S. van der Zwaag, W. A. Groen, *Smart Materials and Structures* **2014** , *23* , 055001.
- [181] H. Gong, Y. Gao, S. Jiang, F. Sun, *ACS Appl Mater Interfaces* **2018** , *10* , 26694-26704.
- [182] X. Li, M. Rui, J. Song, Z. Shen, H. Zeng, *Advanced Functional Materials* **2015** , *25* , 4929-4947.
- [183] F. Liu, M. H. Jang, H. D. Ha, J. H. Kim, Y. H. Cho, T. S. Seo, *Adv Mater* **2013** , *25* , 3657-3662.
- [184] B. Liu, J. Xie, H. Ma, X. Zhang, Y. Pan, J. Lv, H. Ge, N. Ren, H. Su, X. Xie, L. Huang, W. Huang, *Small* **2017** , *13* .
- [185] Y. Li, Y. Hu, Y. Zhao, G. Shi, L. Deng, Y. Hou, L. Qu, *Adv Mater* **2011** , *23* , 776-780.
- [186] Y. W. Han, C. H. Jung, H. S. Lee, S. J. Jeon, D. K. Moon, *ACS Appl Mater Interfaces* **2020** , *12* , 38470-38482.
- [187] H.-J. Wang, T.-T. Yu, H.-L. Chen, W.-B. Nan, L.-Q. Xie, Q.-Q. Zhang, *Dyes and Pigments* **2018** , *159* , 245-251.
- [188] J. Wang, M. Yi, Y. Xin, Y. Pang, Y. Zou, *ACS Appl Mater Interfaces* **2022** , *14* , 48976-48985.
- [189] M. Yi, J. Wang, A. Li, Y. Xin, Y. Pang, Y. Zou, *Advanced Materials Technologies* **2023** , 2201939.